


Encounter-based approach to the escape problem

Denis S. Grebenkov ^{*}

*Laboratoire de Physique de la Matière Condensée, CNRS–Ecole Polytechnique,
Institut Polytechnique de Paris, 91120 Palaiseau, France*

 (Received 21 January 2023; accepted 23 March 2023; published 13 April 2023)

We revise the encounter-based approach to imperfect diffusion-controlled reactions, which employs the statistics of encounters between a diffusing particle and the reactive region to implement surface reactions. We extend this approach to deal with a more general setting, in which the reactive region is surrounded by a reflecting boundary with an escape region. We derive a spectral expansion for the full propagator and investigate the behavior and probabilistic interpretations of the associated probability flux density. In particular, we obtain the joint probability density of the escape time and the number of encounters with the reactive region before escape, and the probability density of the first-crossing time of a prescribed number of encounters. We briefly discuss generalizations of the conventional Poissonian-type surface reaction mechanism described by Robin boundary condition and potential applications of this formalism in chemistry and biophysics.

DOI: [10.1103/PhysRevE.107.044105](https://doi.org/10.1103/PhysRevE.107.044105)

I. INTRODUCTION

Diffusion-controlled reactions play an important role for various chemical and biophysical applications [1–6]. In a typical setting, a particle diffuses inside a confining domain Ω toward a target region, on which it can react or trigger a specific event. One can think of a protein searching for a specific site on a DNA molecule, or a molecule in a chemical reactor searching for a catalytic germ to be transformed. Such diffusion-controlled reactions are often described in terms of the first-passage time to the target or, more generally, to the reaction event [7–15]. The diffusive dynamics of a single molecule is usually characterized by a propagator, $G_q(\mathbf{x}, t|\mathbf{x}_0)$, i.e., the probability density that a molecule started from \mathbf{x}_0 at time 0 has arrived in a vicinity of point \mathbf{x} at a later time t , without being reacted [7,16,17]. For ordinary diffusion, the propagator satisfies the diffusion (or heat) equation,

$$\partial_t G_q(\mathbf{x}, t|\mathbf{x}_0) = D\Delta G_q(\mathbf{x}, t|\mathbf{x}_0) \quad (\mathbf{x} \in \Omega), \quad (1)$$

subject to the initial condition $G_q(\mathbf{x}, 0|\mathbf{x}_0) = \delta(\mathbf{x} - \mathbf{x}_0)$ with a Dirac distribution $\delta(\mathbf{x} - \mathbf{x}_0)$, where D is the diffusion coefficient of the molecule, and Δ is the Laplace operator (the meaning of the subscript q will be explained below). In turn, the reactive properties of the boundary of the confining domain are usually incorporated through the Robin boundary condition,

$$-D\partial_n G_q(\mathbf{x}, t|\mathbf{x}_0) = \kappa(\mathbf{x}) G_q(\mathbf{x}, t|\mathbf{x}_0) \quad (\mathbf{x} \in \partial\Omega), \quad (2)$$

where ∂_n is the normal derivative on the boundary, oriented outwards the confining domain, and $\kappa(\mathbf{x})$ is the reactivity at a boundary point \mathbf{x} . This condition, which was put forward in chemical physics by Collins and Kimball [18] and broadly employed afterwards [19–36], *postulates* that the

diffusive flux from the bulk (the left-hand side) is proportional to the propagator on the boundary. Depending on the type of surface reaction, the proportionality coefficient $\kappa(\mathbf{x})$ (in units m/s) is called reactivity, permeability, or surface relaxivity. In the context of bimolecular reactions, it can also be related to the forward reaction constant. The reactivity $\kappa(\mathbf{x})$ can range from 0 for inert impermeable boundary to $+\infty$ for a perfectly reactive boundary, on which the reaction occurs upon the first arrival of the particle onto that boundary.

A space-dependent reactivity $\kappa(\mathbf{x})$ allows one to implement heterogeneous patterns on a catalytic surface or to describe in a unified way the effects of reactive targets and restricting inert boundaries of a porous medium. However, theoretical description of such general diffusion-controlled reactions is rather challenging (see Ref. [37] and references therein). For this reason, one often focuses on a simpler yet relevant setting of a constant or piecewise constant reactivity. If $\kappa(\mathbf{x})$ is constant, then one can employ standard spectral expansions over the eigenfunctions of the Laplace operator [7,16,17]. Moreover, for simple confining domains such as spheres or parallelepipeds, these eigenfunctions are known exactly that facilitates the analysis of diffusion-controlled reactions [38–41]. Another common setting is the case of a reactive target surrounded by a reflecting boundary so that $\kappa(\mathbf{x}) = \kappa$ on the target surface, and $\kappa(\mathbf{x}) = 0$ on the reflecting boundary. In this case, one deals with mixed Robin-Neumann (or Dirichlet-Neumann for $\kappa = \infty$) boundary conditions. When the target is small, one can employ powerful asymptotic tools to approximate various quantities such as, for instance, the mean reaction time on the target or the decay rate of the survival probability [42–56]. Moreover, if the target is interpreted as a “hole” in the otherwise reflecting impenetrable boundary, then one speaks about the escape or exit problem. As the reaction is understood here as an escape event, the reaction time is called the escape or exit time. Finally, if

^{*}denis.grebenkov@polytechnique.edu

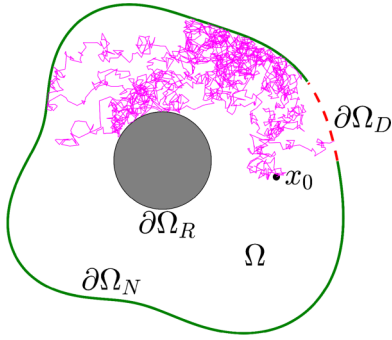


FIG. 1. Illustration of a confining domain Ω whose boundary $\partial\Omega$ is split into three disjoint parts: a target region $\partial\Omega_R$ (the boundary of an obstacle shadowed in gray, e.g., a catalytic germ), a reflecting region $\partial\Omega_N$ (solid green line), and an escape region $\partial\Omega_D$ (dashed red line). A simulated trajectory of a particle that started from a point x_0 and diffused until its escape, is shown in magenta. The particle is always reflected from $\partial\Omega_N$ but may either be reflected from or react on $\partial\Omega_R$.

there are many targets, then their competition for trapping the diffusing particle can be characterized by splitting probabilities [57–63].

In this paper, we consider a more general situation, in which the boundary $\partial\Omega$ of the confining domain is split into three disjoint parts,

$$\partial\Omega = \partial\Omega_R \cup \partial\Omega_N \cup \partial\Omega_D, \quad (3)$$

which represent the reactive target $\partial\Omega_R$, the inert reflecting boundary $\partial\Omega_N$ and the escape region $\partial\Omega_D$ (Fig. 1). In this way, one can describe an important class of diffusion-controlled reactions, in which the diffusing particle can leave the confining domain through an escape region or be destroyed on it, without being reacted on the target region. This is a common setting for many biochemical reactions inside a living cell; for instance, proteins can be disassembled before finding their receptors, while ions can leave the cytoplasm through the ion channels on the plasma membrane. We assume that the particle disappears immediately after the first arrival on the escape region $\partial\Omega_D$. In mathematical terms, such a composed boundary can be implemented through the mixed Robin-Dirichlet-Neumann boundary conditions:

$$\partial_n G_q(\mathbf{x}, t|\mathbf{x}_0) + qG_q(\mathbf{x}, t|\mathbf{x}_0) = 0 \quad (\mathbf{x} \in \partial\Omega_R), \quad (4a)$$

$$G_q(\mathbf{x}, t|\mathbf{x}_0) = 0 \quad (\mathbf{x} \in \partial\Omega_D), \quad (4b)$$

$$\partial_n G_q(\mathbf{x}, t|\mathbf{x}_0) = 0 \quad (\mathbf{x} \in \partial\Omega_N), \quad (4c)$$

where $q = \kappa/D$ is proportional to the (constant) reactivity κ of the target region $\partial\Omega_R$ (note that the subscript of $\partial\Omega_R$, $\partial\Omega_D$ and $\partial\Omega_N$ refers to the corresponding type of Robin, Dirichlet and Neumann boundary condition). Alternatively, these conditions can describe a two-target problem: a partially reactive target $\partial\Omega_R$ and a perfectly reactive target $\partial\Omega_D$ (“reaction” on $\partial\Omega_D$ is interpreted here as the escape event). However, as we focus on reactions on the target region $\partial\Omega_R$, we keep speaking about a single-target problem in the presence of escape events.

To solve this problem, one could still introduce the Laplacian eigenfunctions that satisfy the same mixed boundary conditions. Here we follow an alternative way and generalize

the encounter-based approach that was developed in Ref. [64] for the particular case of a constant reactivity on the whole boundary (when $\partial\Omega = \partial\Omega_R$ and $\partial\Omega_N = \partial\Omega_D = \emptyset$). This approach relies on the concept of the boundary local time ℓ_t , which can represent a rescaled number of encounters between the diffusing particle and the boundary up to time t . In this way, one can first investigate the diffusive dynamics inside a confining domain with reflecting boundary and then implement surface reactions explicitly (see below). Moreover, one can go beyond the conventional Poissonian-type reactions described by Robin boundary condition (4a) and implement saturation or activation effects or, more generally, encounter-dependent reactivity [64]. Our generalization allows one to investigate the effects of the escape event onto such reactions. We also provide probabilistic interpretations of the probability flux density that were not discussed enough in earlier works. In particular, we obtain the joint probability density of the position, boundary local time and the escape time.

The paper is organized as follows. In Sec. II, we present the main theoretical results. After introducing the necessary elements of the conventional and encounter-based approaches in Secs. II A and II B, we discuss the distribution of the boundary local time (Sec. II C) and restrictions of the probability flux density to $\partial\Omega_D$ and $\partial\Omega_R$ (Secs. II D and II E). In Sec. III, we illustrate the behavior of the derived quantities for a particle diffusing between two concentric spheres. In this case, all the “ingredients” of the encounter-based approach can be found explicitly. Section IV presents further discussions, conclusions and perspectives.

II. MAIN RESULTS

A. Conventional approach

To highlight the advantages of the encounter-based approach, we briefly recall several characteristics of diffusion-controlled reactions accessed within the conventional approach that relies on the propagator $G_q(\mathbf{x}, t|\mathbf{x}_0)$. We consider a pointlike particle diffusing in a bounded Euclidean domain $\Omega \subset \mathbb{R}^d$ with smooth boundary $\partial\Omega$, which is partitioned into reactive ($\partial\Omega_R$), reflecting ($\partial\Omega_N$), and escape ($\partial\Omega_D$) parts. As the diffusing particle can disappear due to either escape through $\partial\Omega_D$ or reaction on $\partial\Omega_R$, one can naturally introduce two first-passage times: the escape time

$$T_q = \inf\{t > 0 : X_t \in \partial\Omega_D\} \quad (5)$$

as the first-passage time to the escape region $\partial\Omega_D$, and the reaction time τ_q as the random instance of the reaction event on $\partial\Omega_R$ (its formal definition is nontrivial and will be given in Sec. II E). The subscript q highlights that the distributions of both random variables T_q and τ_q depend on the reactivity of the target region because they are determined by the probability flux density,

$$j_q(\mathbf{x}, t|\mathbf{x}_0) = -D\partial_n G_q(\mathbf{x}, t|\mathbf{x}_0) \quad (\mathbf{x} \in \partial\Omega). \quad (6)$$

In fact, the restriction of $j_q(\mathbf{x}, t|\mathbf{x}_0)$ to the escape region $\partial\Omega_D$ is the joint probability density of the escape location X_{T_q} and its time T_q . In turn, the restriction of $j_q(\mathbf{x}, t|\mathbf{x}_0)$ to the target region $\partial\Omega_R$ is the joint probability density of the reaction location X_{τ_q} and its time τ_q [note that the restriction of $j_q(\mathbf{x}, t|\mathbf{x}_0)$

to $\partial\Omega_N$ is strictly zero due to the Neumann boundary condition (4c)]. If the position does not matter, then it can be averaged out to get the (marginal) probability densities of the escape time T_q and of the reaction time τ_q :

$$J_q^D(t|\mathbf{x}_0) = \int_{\partial\Omega_D} d\mathbf{x} j_q(\mathbf{x}, t|\mathbf{x}_0), \quad (7a)$$

$$J_q^R(t|\mathbf{x}_0) = \int_{\partial\Omega_R} d\mathbf{x} j_q(\mathbf{x}, t|\mathbf{x}_0). \quad (7b)$$

As the particle can either escape or react, none of these densities is normalized to 1; in turn, one has

$$\int_0^\infty dt [J_q^D(t|\mathbf{x}_0) + J_q^R(t|\mathbf{x}_0)] = 1. \quad (8)$$

To show this normalization, one can integrate the diffusion equation (1) over $\mathbf{x} \in \Omega$ and use the Green's formula and mixed boundary conditions (4) to get the continuity equation

$$\partial_t S_q(t|\mathbf{x}_0) = -[J_q^D(t|\mathbf{x}_0) + J_q^R(t|\mathbf{x}_0)], \quad (9)$$

where

$$S_q(t|\mathbf{x}_0) = \int_\Omega d\mathbf{x} G_q(\mathbf{x}, t|\mathbf{x}_0) \quad (10)$$

is the survival probability of the particle up to time t . The integral of Eq. (9) over t from 0 to infinity yields the normalization (8), given that $S_q(0|\mathbf{x}_0) = 1$ and $S_q(t|\mathbf{x}_0) \rightarrow 0$ as $t \rightarrow \infty$ for diffusion in a bounded domain.

B. Encounter-based approach

In the encounter-based approach, one first characterizes purely diffusive dynamics inside a bounded confining domain Ω with a *reflecting* boundary $\partial\Omega$, and then incorporates surface reactions on $\partial\Omega$, i.e., transforms the reflecting boundary into the reactive one [64]. For this purpose, one uses the boundary local time ℓ_t , which was first introduced by Lévy [65] and then extensively employed in mathematical literature on stochastic processes [66,67]. The boundary local time can be defined as the renormalized residence time near the boundary $\partial\Omega$:

$$\ell_t = \lim_{a \rightarrow 0} \frac{D}{a} \int_0^t dt' \Theta(a - |\mathbf{X}_{t'} - \partial\Omega|), \quad (11)$$

where $|\mathbf{X}_{t'} - \partial\Omega|$ is the Euclidean distance between the position $\mathbf{X}_{t'}$ of the particle at time t' and the boundary $\partial\Omega$, and $\Theta(z)$ is the Heaviside step function: $\Theta(z) = 1$ for $z > 0$ and 0 otherwise. The integral in Eq. (11) defines the residence (also known as occupation or sojourn) time in a thin layer of width a near the boundary. As the boundary $\partial\Omega$ has a lower dimension as compared to the domain Ω , the residence time vanishes as the layer shrinks (when $a \rightarrow 0$); in turn, its renormalization by a yields the nontrivial limit (11). The boundary local time should not be confused with the local time in a bulk point, which has been intensively studied, especially for diffusive processes in one dimension [68,69]. Despite its name, the boundary local time has units of length. The boundary local time can be equivalently defined as a rescaled limit of the number \mathcal{N}_t^a of downcrossings of the boundary layer of width a up to time t : $\ell_t = \lim_{a \rightarrow 0} a \mathcal{N}_t^a$. As each downcrossing can be interpreted as an encounter of the particle with the boundary,

the boundary local time ℓ_t characterizes the statistics of such encounters [70]. The diffusive dynamics can then be described either by a stochastic differential equation for the random pair (\mathbf{X}_t, ℓ_t) , or by the so-called full propagator $P(\mathbf{x}, \ell, t|\mathbf{x}_0)$, i.e., the joint probability density of getting the values (\mathbf{x}, ℓ) for the pair (\mathbf{X}_t, ℓ_t) . Once the full propagator is known, one can implement various surface reaction mechanisms (see Sec. II E).

By construction, the boundary local time ℓ_t characterizes encounters with the whole boundary $\partial\Omega$ that does not allow one to implement different reaction mechanisms on different subsets of the boundary. This problem has been discussed and partly resolved in Ref. [71] by introducing a proper boundary local time ℓ_t^i on each subset of interest. In this case, one would deal with the joint probability density for \mathbf{X}_t and for boundary local times on all these subsets. Even though a formal way for computing this density was proposed in Ref. [71], its practical implementation was realized only for simple geometric settings (e.g., an interval).

In the context of the escape problem that we consider in this paper, one can follow a different strategy. As we are interested in describing reactions exclusively on the target region $\partial\Omega_R$, we need to know the statistics of encounters with that particular region. In other words, one can modify the above definition of the boundary local time to count encounters only with $\partial\Omega_R$:

$$\ell_t^R = \lim_{a \rightarrow 0} \frac{D}{a} \int_0^t dt' \Theta(a - |\mathbf{X}_{t'} - \partial\Omega_R|). \quad (12)$$

This relation defines a nondecreasing stochastic process ℓ_t^R (starting from $\ell_0^R = 0$) that increases at each encounter with $\partial\Omega_R$. As previously, the integral is the residence time that a particle spent in a thin layer of width a near the target region $\partial\Omega_R$ up to time t . When a is small, this residence time can thus be approximated as $\ell_t^R a/D$ according to Eq. (12). In the same vein, we introduce the full propagator $P(\mathbf{x}, \ell, t|\mathbf{x}_0)$ as the joint probability density for \mathbf{X}_t and ℓ_t^R (not ℓ_t), under the condition of no escape through $\partial\Omega_D$ up to time t . As previously, the target region $\partial\Omega_R$ is treated at this step as *reflecting*, i.e., the particle described by the full propagator can disappear only on the escape region $\partial\Omega_D$.

At the next step, one can introduce reaction events on $\partial\Omega_R$ following the probabilistic arguments from Ref. [64]. For this purpose, one can consider a thin reactive layer of width a near the target region $\partial\Omega_R$. Once the particle enters this layer, surface reaction may be described by a standard first-order reaction kinetics, with the rate $k = \kappa/a$. Since the residence time of the particle within this layer up to time t is approximately equal to $\ell_t^R a/D$, the probability of no reaction on $\partial\Omega_R$ up to t is then $e^{-k(\ell_t^R a/D)} = e^{-q\ell_t^R}$, where $q = \kappa/D$. As a consequence, one deduces the following relation between the conventional and full propagators:

$$\begin{aligned} G_q(\mathbf{x}, t|\mathbf{x}_0) &= \mathbb{E}_{\mathbf{x}_0} \{ \delta(\mathbf{X}_t - \mathbf{x}) e^{-q\ell_t^R} \Theta(T_q - t) \} \\ &= \int_0^\infty d\ell e^{-q\ell} P(\mathbf{x}, \ell, t|\mathbf{x}_0). \end{aligned} \quad (13)$$

On the left-hand side, the conventional propagator $G_q(\mathbf{x}, t|\mathbf{x}_0)$ satisfying Eqs. (1) and (4), describes diffusion from \mathbf{x}_0 to \mathbf{x} in time t , under the condition of no escape through $\partial\Omega_D$ and no reaction on $\partial\Omega_R$ up to t . The probability density of this event

can be written via the expectation in the middle, i.e., as the fraction of trajectories X_t of reflected Brownian motion between \mathbf{x}_0 and \mathbf{x} of duration t , with the penalizing factor $e^{-q\ell_t^R}$ eliminating a subset of trajectories that reacted on $\partial\Omega_R$, while $\Theta(T_q - t)$ eliminating those that have escaped before t . On the right-hand side, the full propagator $P(\mathbf{x}, \ell, t|\mathbf{x}_0)$ describes diffusion from \mathbf{x}_0 to \mathbf{x} in time t , under the condition of no escape through $\partial\Omega_D$ and of getting the boundary local time ℓ_t^R equal to ℓ . In turn, the factor $e^{-q\ell}$ incorporates the probability of no reaction on $\partial\Omega_R$ for any realized value ℓ of the boundary local time ℓ_t^R , while the integral over ℓ sums up contributions from all possible realizations of ℓ_t^R . In other words, this integral simply evaluates the expectation in the middle. We stress that the condition $T_q > t$ of no escape through $\partial\Omega_D$ is implemented in the full propagator $P(\mathbf{x}, \ell, t|\mathbf{x}_0)$ through the Dirichlet boundary condition on $\partial\Omega_D$ (see below).

The relation (13) plays the central role in this work. On the one hand, it allows one to incorporate the conventional surface reactions as the Laplace transform of the full propagator $P(\mathbf{x}, \ell, t|\mathbf{x}_0)$ with respect to ℓ . Importantly, the reactivity parameter q enters *explicitly* through the exponential factor $e^{-q\ell}$, whereas it appeared *implicitly* in the conventional description as a coefficient in Robin boundary condition (4a). Finally, one can replace the factor $e^{-q\ell}$, which is reminiscent of an exponential probability law, by another function, allowing one to implement various surface reaction mechanisms (see Sec. II E). On the other hand, the inverse Laplace transform of the conventional propagator $G_q(\mathbf{x}, t|\mathbf{x}_0)$ with respect to q gives access to the full propagator:

$$P(\mathbf{x}, \ell, t|\mathbf{x}_0) = \mathcal{L}_{q \rightarrow \ell}^{-1}\{G_q(\mathbf{x}, t|\mathbf{x}_0)\}. \quad (14)$$

Unfortunately, an implicit dependence of $G_q(\mathbf{x}, t|\mathbf{x}_0)$ on q often prevents using this inversion and thus urges for another representation for the full propagator.

To achieve this goal, we extend the spectral expansion of the full propagator developed in Ref. [64]. For this purpose, we introduce an extension of the so-called Dirichlet-to-Neumann operator \mathcal{M}_p that associates to a given function f on the target region $\partial\Omega_R$ another function g on that region such that

$$\mathcal{M}_p f = g = (\partial_n u)|_{\partial\Omega_R}, \quad (15)$$

where u is the solution of the following boundary value problem with $p \geq 0$:

$$(p - D\Delta)u = 0 \quad (\mathbf{x} \in \Omega), \quad (16a)$$

$$u = f \quad (\mathbf{x} \in \partial\Omega_R), \quad (16b)$$

$$u = 0 \quad (\mathbf{x} \in \partial\Omega_D), \quad (16c)$$

$$\partial_n u = 0 \quad (\mathbf{x} \in \partial\Omega_N). \quad (16d)$$

In other words, the operator \mathcal{M}_p transforms the Dirichlet boundary condition $u = f$ on $\partial\Omega_R$ into an equivalent Neumann boundary condition $\partial_n u = g$ on $\partial\Omega_R$, keeping unchanged the Dirichlet and Neumann conditions on $\partial\Omega_D$ and $\partial\Omega_N$ respectively. While the conventional Dirichlet-to-Neumann operator acted on functions on the whole boundary $\partial\Omega$, our extension acts on functions on the subset $\partial\Omega_R$ of the boundary. The spectral properties of the conventional Dirichlet-to-Neumann operator have been intensively studied

in mathematical literature [72–78]. Most of these properties are expected to be valid for our extension so that \mathcal{M}_p is a pseudo-differential self-adjoint operator. Since the target region $\partial\Omega_R$ is bounded, the spectrum of \mathcal{M}_p is discrete, with an infinite set of positive eigenvalues $\mu_k^{(p)}$ ($k = 0, 1, 2, \dots$), that can be enumerated in the increasing order:

$$0 \leq \mu_0^{(p)} \leq \mu_1^{(p)} \leq \dots \leq \mu_k^{(p)} \leq \dots \nearrow +\infty. \quad (17)$$

In turn, the associated eigenfunctions $v_k^{(p)}(\mathbf{x})$ form a complete orthonormal basis of the functional space $L_2(\partial\Omega_R)$ of square integrable functions on $\partial\Omega_R$. A rigorous formulation and demonstration of these mathematical properties are beyond the scope of this paper. From the mathematical point of view, one can consider them as conjectural extensions of the well-known conventional case.

The eigenbasis of the Dirichlet-to-Neumann operator can serve for getting a spectral expansion of the full propagator. Skipping technical details (given in Ref. [64]), we sketch here the main steps of this derivation. In the first step, the Laplace transform of the conventional propagator $G_q(\mathbf{x}, t|\mathbf{x}_0)$ with respect to time t ,

$$\tilde{G}_q(\mathbf{x}, p|\mathbf{x}_0) = \int_0^\infty dt e^{-pt} G_q(\mathbf{x}, t|\mathbf{x}_0), \quad (18)$$

reduces the diffusion equation (1) to the inhomogeneous modified Helmholtz equation:

$$(p - D\Delta)\tilde{G}_q(\mathbf{x}, p|\mathbf{x}_0) = \delta(\mathbf{x} - \mathbf{x}_0), \quad (19)$$

subject to the same boundary condition (here and below, tilde denotes Laplace-transformed quantities with respect to t). Writing $\tilde{G}_q(\mathbf{x}, p|\mathbf{x}_0) = \tilde{G}_\infty(\mathbf{x}, p|\mathbf{x}_0) + \tilde{g}_q(\mathbf{x}, p|\mathbf{x}_0)$ with an unknown function $\tilde{g}_q(\mathbf{x}, p|\mathbf{x}_0)$, one eliminates $\delta(\mathbf{x} - \mathbf{x}_0)$ from the right-hand side. As $\tilde{g}_q(\mathbf{x}, p|\mathbf{x}_0)$ satisfies $(p - D\Delta)\tilde{g}_q(\mathbf{x}, p|\mathbf{x}_0) = 0$, one can employ the eigenfunctions of \mathcal{M}_p for a spectral decomposition of the restriction of $\tilde{g}_q(\mathbf{x}, p|\mathbf{x}_0)$ to $\partial\Omega_R$, which can then be extended to the whole domain Ω . Finally, one takes the inverse Laplace transform of $\tilde{G}_q(\mathbf{x}, p|\mathbf{x}_0)$ with respect to q to get the spectral expansion of the full propagator in the Laplace domain:

$$\begin{aligned} \tilde{P}(\mathbf{x}, \ell, p|\mathbf{x}_0) &= \tilde{G}_\infty(\mathbf{x}, p|\mathbf{x}_0)\delta(\ell) \\ &+ \frac{1}{D} \sum_{k=0}^{\infty} [V_k^{(p)}(\mathbf{x}_0)]^* V_k^{(p)}(\mathbf{x}) e^{-\mu_k^{(p)}\ell}, \end{aligned} \quad (20)$$

where asterisk denotes complex conjugate, and

$$V_k^{(p)}(\mathbf{x}_0) = \int_{\partial\Omega_R} d\mathbf{x} \tilde{j}_\infty(\mathbf{x}, p|\mathbf{x}_0) v_k^{(p)}(\mathbf{x}) \quad (21)$$

is the extension of the eigenfunction $v_k^{(p)}(\mathbf{x})$ (defined on $\partial\Omega_R$) to the whole domain Ω . While the structure of the spectral expansion (20) is identical to that derived in Ref. [64], its “ingredients” $\tilde{G}_\infty(\mathbf{x}, p|\mathbf{x}_0)$, $V_k^{(p)}(\mathbf{x}_0)$, and $\mu_k^{(p)}$ are adapted to account for the presence of reflecting and escape regions.

One can easily check that the functions $V_k^{(p)}(\mathbf{x})$ defined by Eq. (21) satisfy

$$(p - D\Delta)V_k^{(p)}(\mathbf{x}) = 0 \quad (\mathbf{x} \in \Omega), \quad (22a)$$

$$V_k^{(p)}(\mathbf{x}) = v_k^{(p)}(\mathbf{x}) \quad (\mathbf{x} \in \partial\Omega_R), \quad (22b)$$

$$V_k^{(p)}(\mathbf{x}) = 0 \quad (\mathbf{x} \in \partial\Omega_D), \quad (22c)$$

$$\partial_n V_k^{(p)}(\mathbf{x}) = 0 \quad (\mathbf{x} \in \partial\Omega_N). \quad (22d)$$

Moreover, since $v_k^{(p)}$ is an eigenfunction of the Dirichlet-to-Neumann operator, one has

$$\partial_n V_k^{(p)}(\mathbf{x}) = \mu_k^{(p)} V_k^{(p)}(\mathbf{x}) = \mu_k^{(p)} v_k^{(p)}(\mathbf{x}) \quad (\mathbf{x} \in \partial\Omega_R). \quad (23)$$

Once the eigenfunction $v_k^{(p)}$ is found, one can determine its extension $V_k^{(p)}(\mathbf{x})$ either via Eq. (21), or by solving the above problem (22). Alternatively, without knowing $v_k^{(p)}$, one can look directly at the eigenvalue problems (22a), (22c), (22d), and (23), in which the spectral parameter (here, $\mu_k^{(p)}$) stands in the boundary condition. This is known as the Steklov problem (see Ref. [78] and references therein), while $\mu_k^{(p)}$ and $V_k^{(p)}(\mathbf{x})$ are the eigenvalues and eigenfunctions of this problem. Despite this equivalence, we keep referring to the Dirichlet-to-Neumann operator \mathcal{M}_p and its spectral properties.

The inverse Laplace transform of Eq. (20) with respect to p formally yields

$$P(\mathbf{x}, \ell, t|\mathbf{x}_0) = G_\infty(\mathbf{x}, t|\mathbf{x}_0)\delta(\ell) + \mathcal{L}_{p \rightarrow t}^{-1} \left\{ \frac{1}{D} \sum_{k=0}^{\infty} [V_k^{(p)}(\mathbf{x}_0)]^* V_k^{(p)}(\mathbf{x}) e^{-\mu_k^{(p)} \ell} \right\}. \quad (24)$$

The first term in Eq. (24) represents the contribution of random trajectories from \mathbf{x}_0 to \mathbf{x} of duration t without hitting neither the target region $\partial\Omega_R$, nor the escape region $\partial\Omega_D$ (in turn, they could encounter the reflecting part $\partial\Omega_N$). Their “fraction” is precisely given by $G_\infty(\mathbf{x}, t|\mathbf{x}_0)$, with Dirichlet boundary condition on $\partial\Omega_D$ and $\partial\Omega_R$ [note that Eq. (4a) becomes $G_\infty(\mathbf{x}, t|\mathbf{x}_0) = 0$ for $q = \infty$]. As the boundary local time ℓ_t^R remained zero for these trajectories, one gets the singular factor $\delta(\ell)$. In turn, the second term accounts for all trajectories that have encountered the target region $\partial\Omega_R$, but still avoided the escape through $\partial\Omega_D$ [the latter condition is implemented via Eq. (22c) for all $V_k^{(p)}(\mathbf{x})$]. The spectral representation (24) is an alternative way for computing the full propagator, which is complementary to Eq. (14). While both expressions involve an inverse Laplace transform, the spectral characteristics of the Dirichlet-to-Neumann operator are in general easier to access than the conventional propagator $G_q(\mathbf{x}, t|\mathbf{x}_0)$ in time domain. For instance, we will employ Eq. (24) in Sec. III to deduce various properties of diffusion-controlled reactions in a spherical domain. We emphasize that two representations provide complementary insights onto the full propagator.

The full propagator determines the corresponding probability flux density on the boundary $\partial\Omega$:

$$j(\mathbf{x}, \ell, t|\mathbf{x}_0) = -D \partial_n P(\mathbf{x}, \ell, t|\mathbf{x}_0) \quad (\mathbf{x} \in \partial\Omega). \quad (25)$$

The spectral expansion (20) gives access to this quantity in the Laplace domain

$$\tilde{j}(\mathbf{x}, \ell, p|\mathbf{x}_0) = \tilde{j}_\infty(\mathbf{x}, p|\mathbf{x}_0)\delta(\ell) - \sum_{k=0}^{\infty} [V_k^{(p)}(\mathbf{x}_0)]^* (\partial_n V_k^{(p)})(\mathbf{x}) e^{-\mu_k^{(p)} \ell}. \quad (26)$$

The probability flux density $j(\mathbf{x}, \ell, t|\mathbf{x}_0)$ is the main object of our study. In particular, we aim at providing its probabilistic interpretation and deducing various related characteristics of diffusion-controlled reactions in the presence of escape events. We will show that the interpretation of $j(\mathbf{x}, \ell, t|\mathbf{x}_0)$ is more subtle than that of $j_q(\mathbf{x}, t|\mathbf{x}_0)$ mentioned in Sec. II A. For instance, it is easy to prove that

$$\int_0^\infty d\ell j(\mathbf{x}, \ell, t|\mathbf{x}_0) = 0 \quad (\mathbf{x} \in \partial\Omega_R), \quad (27)$$

i.e., the restriction of $j(\mathbf{x}, \ell, t|\mathbf{x}_0)$ to $\partial\Omega_R$ is not necessarily positive.

To show this relation, let us first integrate Eq. (20) over ℓ from 0 to infinity to get the following identity:

$$\tilde{G}_0(\mathbf{x}, p|\mathbf{x}_0) = \tilde{G}_\infty(\mathbf{x}, p|\mathbf{x}_0) + \frac{1}{D} \sum_{k=0}^{\infty} [V_k^{(p)}(\mathbf{x}_0)]^* V_k^{(p)}(\mathbf{x}) \frac{1}{\mu_k^{(p)}}, \quad (28)$$

so that

$$\tilde{j}_0(\mathbf{x}, p|\mathbf{x}_0) = \tilde{j}_\infty(\mathbf{x}, p|\mathbf{x}_0) - \sum_{k=0}^{\infty} [V_k^{(p)}(\mathbf{x}_0)]^* (\partial_n V_k^{(p)})(\mathbf{x}) \frac{1}{\mu_k^{(p)}}. \quad (29)$$

For any $\mathbf{x} \in \partial\Omega_R$, the left-hand side of Eq. (29) is zero, implying

$$\tilde{j}_\infty(\mathbf{x}, p|\mathbf{x}_0) = \sum_{k=0}^{\infty} [V_k^{(p)}(\mathbf{x}_0)]^* v_k^{(p)}(\mathbf{x}) \quad (\mathbf{x} \in \partial\Omega_R), \quad (30)$$

where we applied Eq. (23). Using the identity (30), one can easily check that the integral of Eq. (26) over ℓ from 0 to infinity is strictly zero for any $\mathbf{x} \in \partial\Omega_R$, that reads in time domain as Eq. (27).

To clarify the probabilistic meaning of $j(\mathbf{x}, \ell, t|\mathbf{x}_0)$, we first look at the distribution of the boundary local time ℓ_t^R , then discuss the restriction of $j(\mathbf{x}, \ell, t|\mathbf{x}_0)$ to the escape region $\partial\Omega_D$, and finally describe its restriction to the target region $\partial\Omega_R$.

C. Probability density of the boundary local time

It is convenient to start by inspecting the distribution of the boundary local time ℓ_t^R . By definition, the integral of the full propagator $P(\mathbf{x}, \ell, t|\mathbf{x}_0)$ over $\mathbf{x} \in \Omega$ determines the (marginal) probability density of the boundary local time

$$\rho(\ell, t|\mathbf{x}_0) = \int_\Omega d\mathbf{x} P(\mathbf{x}, \ell, t|\mathbf{x}_0). \quad (31)$$

Since the particle may escape the domain, this probability density is not normalized to 1:

$$\int_0^\infty d\ell \rho(\ell, t|\mathbf{x}_0) = S_0(t|\mathbf{x}_0) = \mathbb{P}_{\mathbf{x}_0}\{T_0 > t\}, \quad (32)$$

i.e., the probability of no escape up to time t (the subscript $q = 0$ of T_0 highlights that the target region $\partial\Omega_R$ is treated here as reflecting). Only if there is no escape region, the survival probability $S_0(t|\mathbf{x}_0)$ is equal to 1, ensuring the normalization in the conventional case [79].

Integrating the fundamental relation (13) over $\mathbf{x} \in \Omega$, one gets

$$S_q(t|\mathbf{x}_0) = \int_0^\infty d\ell e^{-q\ell} \rho(\ell, t|\mathbf{x}_0) = \mathbb{E}_{\mathbf{x}_0}\{e^{-q\ell_t^R}\}, \quad (33)$$

i.e., the survival probability is the generating function of ℓ_t^R . Moreover, the inverse Laplace transform of Eq. (9) with respect to q yields another continuity equation

$$\partial_t \rho(\ell, t|\mathbf{x}_0) = -[J_R(\ell, t|\mathbf{x}_0) + J_D(\ell, t|\mathbf{x}_0)], \quad (34)$$

where

$$J_R(\ell, t|\mathbf{x}_0) = \int_{\partial\Omega_R} d\mathbf{x} j(\mathbf{x}, \ell, t|\mathbf{x}_0), \quad (35a)$$

$$J_D(\ell, t|\mathbf{x}_0) = \int_{\partial\Omega_D} d\mathbf{x} j(\mathbf{x}, \ell, t|\mathbf{x}_0), \quad (35b)$$

and we used that

$$j_q(\mathbf{x}, t|\mathbf{x}_0) = \int_0^\infty d\ell e^{-q\ell} j(\mathbf{x}, \ell, t|\mathbf{x}_0) \quad (36)$$

due to Eq. (13).

In the Laplace domain, the integral of Eq. (20) yields

$$\begin{aligned} \tilde{\rho}(\ell, p|\mathbf{x}_0) &= \tilde{S}_\infty(p|\mathbf{x}_0)\delta(\ell) + \frac{1}{D} \sum_{k=0}^{\infty} [V_k^{(p)}(\mathbf{x}_0)]^* e^{-\mu_k^{(p)}\ell} \\ &\times \int_{\Omega} d\mathbf{x} V_k^{(p)}(\mathbf{x}). \end{aligned} \quad (37)$$

D. Escape events

In a direct analogy with $j_q(\mathbf{x}, t|\mathbf{x}_0)$, the restriction of the probability flux density $j(\mathbf{x}, \ell, t|\mathbf{x}_0)$ to the escape region $\partial\Omega_D$ determines the joint probability density of the position \mathbf{X}_{T_0} , the boundary local time $\ell_{T_0}^R$, and the escape time T_0 defined by Eq. (5). If the exact location of the escape does not matter, then one can integrate over $\mathbf{x} \in \partial\Omega_D$ to get the joint probability density $J_D(\ell, t|\mathbf{x}_0)$ of $\ell_{T_0}^R$ and T_0 , see Eq. (35b). In the Laplace domain, this quantity reads

$$\tilde{J}_D(\ell, p|\mathbf{x}_0) = \tilde{J}_\infty^D(p|\mathbf{x}_0)\delta(\ell) + \sum_{k=0}^{\infty} [V_k^{(p)}(\mathbf{x}_0)]^* e^{-\mu_k^{(p)}\ell} C_k^{(p)}, \quad (38)$$

where

$$C_k^{(p)} = - \int_{\partial\Omega_D} d\mathbf{x} \partial_n V_k^{(p)}(\mathbf{x}) \quad (39)$$

and $\tilde{J}_\infty^D(p|\mathbf{x}_0)$ is given by Eq. (7a) at $q = \infty$. While the escape time T_0 has been studied in the past, the joint distribution of $\ell_{T_0}^R$ and T_0 has not been reported earlier.

Integrating Eq. (22a), using the Green's formula and expressions (22d), (23), one gets another representation:

$$C_k^{(p)} = \mu_k^{(p)} \int_{\partial\Omega_R} d\mathbf{x} v_k^{(p)}(\mathbf{x}) - \frac{p}{D} \int_{\Omega} d\mathbf{x} V_k^{(p)}(\mathbf{x}). \quad (40)$$

One can apply this representation to check the correct normalization of $J_D(\ell, t|\mathbf{x}_0)$:

$$\begin{aligned} \int_0^\infty d\ell \int_0^\infty dt J_D(\ell, t|\mathbf{x}_0) &= \int_0^\infty d\ell \tilde{J}_D(\ell, 0|\mathbf{x}_0) \\ &= \tilde{J}_\infty^D(0|\mathbf{x}_0) + \sum_{k=0}^{\infty} [V_k^{(0)}(\mathbf{x}_0)]^* \frac{C_k^{(0)}}{\mu_k^{(0)}} \\ &= \tilde{J}_\infty^D(0|\mathbf{x}_0) + \tilde{J}_\infty^R(0|\mathbf{x}_0) = 1, \end{aligned}$$

where we used Eq. (30). The last equality follows from that the fact that $\tilde{J}_\infty^D(0|\mathbf{x}_0)$ and $\tilde{J}_\infty^R(0|\mathbf{x}_0)$ are the splitting probabilities (e.g., $\tilde{J}_\infty^D(0|\mathbf{x}_0)$ is the probability of hitting $\partial\Omega_D$ before hitting $\partial\Omega_R$) so that their sum is equal to 1.

The integral of $J_D(\ell, t|\mathbf{x}_0)$ over ℓ determines the (marginal) probability density function of the escape time T_0

$$J_0^D(t|\mathbf{x}_0) = \int_0^\infty d\ell J_D(\ell, t|\mathbf{x}_0). \quad (41)$$

Integrating the continuity relation (34) over ℓ from 0 to infinity and using the identity (27), one sees that

$$\partial_t S_0(t|\mathbf{x}_0) = -J_0^D(t|\mathbf{x}_0), \quad (42)$$

where we also used the normalization (32). We thus re-derived that the probability density of the first-passage time to $\partial\Omega_D$ is obtained as the negative time derivative of the survival probability $S_0(t|\mathbf{x}_0)$. Expectedly, the derivation of this classical quantity does not require the encounter-based approach.

In turn, the integral of $J_D(\ell, t|\mathbf{x}_0)$ over t yields the (marginal) probability density of the boundary local time $\ell_{T_0}^R$ acquired before the escape:

$$\begin{aligned} \rho_D(\ell|\mathbf{x}_0) &= \int_0^\infty dt J_D(\ell, t|\mathbf{x}_0) = \tilde{J}_D(\ell, 0|\mathbf{x}_0) \\ &= \tilde{J}_\infty^D(0|\mathbf{x}_0)\delta(\ell) + \sum_{k=0}^{\infty} [V_k^{(0)}(\mathbf{x}_0)]^* e^{-\mu_k^{(0)}\ell} C_k^{(0)}. \end{aligned} \quad (43)$$

Here, the first term accounts for the trajectories that never hit the target region $\partial\Omega_R$ and moved directly to the escape region [with the splitting probability $\tilde{J}_\infty^D(0|\mathbf{x}_0)$] so that the acquired boundary local time is zero. In turn, the second term includes the contribution of remaining trajectories.

The expression (38) allows one to determine joint positive integer-order moments of $\ell_{T_0}^R$ and T_0 as

$$\mathbb{E}_{\mathbf{x}_0}\{[\ell_{T_0}^R]^m T_0^n\} = (-1)^n m! \lim_{p \rightarrow 0} \frac{\partial^n}{\partial p^n} \sum_{k=0}^{\infty} \frac{[V_k^{(p)}(\mathbf{x}_0)]^* C_k^{(p)}}{[\mu_k^{(p)}]^{m+1}} \quad (44)$$

for any $m = 1, 2, \dots$ and any $n = 0, 1, \dots$ [for $m = 0$, the contribution from the first (singular) term in Eq. (38) has to be included]. In this way, one can evaluate not only the moments of $\ell_{T_0}^R$ and T_0 , but also correlations between them. In particular,

the mean of $\ell_{T_0}^R$ reads

$$\begin{aligned}\mathbb{E}_{\mathbf{x}_0}\{\ell_{T_0}^R\} &= \sum_{k=0}^{\infty} [V_k^{(0)}(\mathbf{x}_0)]^* \frac{C_k^{(0)}}{[\mu_k^{(0)}]^2} \\ &= \sum_{k=0}^{\infty} [V_k^{(0)}(\mathbf{x}_0)]^* \frac{1}{\mu_k^{(0)}} \int_{\partial\Omega_R} d\mathbf{x} v_k^{(0)}(\mathbf{x}) \\ &= \int_{\partial\Omega_R} d\mathbf{x} D\tilde{G}_0(\mathbf{x}, 0|\mathbf{x}_0),\end{aligned}\quad (45)$$

where we used the identity (28). This result is rather intuitive. In fact, the Green's function $D\tilde{G}_0(\mathbf{x}, 0|\mathbf{x}_0)$ is known to be the mean residence time of Brownian motion in a point \mathbf{x} before the escape [80]. The integral of this quantity over a thin layer of width a near the target region $\partial\Omega_R$ yields the mean residence time in this layer, while the rescaling by D/a results in the mean boundary local time in the limit $a \rightarrow 0$; see Eq. (11).

To evaluate higher-order moments, we first integrate Eq. (20) $m+1$ times to get

$$\begin{aligned}&\sum_{k=0}^{\infty} \frac{[V_k^{(p)}(\mathbf{x}_0)]^* V_k^{(p)}(\mathbf{x})}{[\mu_k^{(p)}]^{m+1}} \\ &= \int_0^{\infty} d\ell_1 \int_{\ell_1}^{\infty} d\ell_2 \dots \int_{\ell_{m+1}}^{\infty} d\ell_{m+1} D\tilde{P}(\mathbf{x}, \ell_{m+1}, p|\mathbf{x}_0) \\ &= \frac{1}{m!} \int_0^{\infty} d\ell \ell^m D\tilde{P}(\mathbf{x}, \ell, p|\mathbf{x}_0)\end{aligned}\quad (46)$$

for any $m = 1, 2, \dots$. In turn, differentiating m times the fundamental relation (13) with respect to q , we derive the following identity:

$$\sum_{k=0}^{\infty} \frac{[V_k^{(p)}(\mathbf{x}_0)]^* V_k^{(p)}(\mathbf{x})}{[\mu_k^{(p)}]^{m+1}} = \frac{(-1)^m}{m!} \lim_{q \rightarrow 0} \partial_q^m D\tilde{G}_q(\mathbf{x}, p|\mathbf{x}_0) \quad (47)$$

for $m = 1, 2, \dots$ [for $m = 0$, there is an additional term, see Eq. (28)]. This identity provides a peculiar interpretation of the derivatives of the Green's function $\tilde{G}_q(\mathbf{x}, p|\mathbf{x}_0)$ with respect to q . Using Eqs. (39), (44), one gets

$$\begin{aligned}\mathbb{E}_{\mathbf{x}_0}\{[\ell_{T_0}^R]^m T_0^n\} &= \frac{(-1)^{m+n+1}}{m!} \\ &\quad \times \lim_{\substack{q \rightarrow 0 \\ p \rightarrow 0}} \partial_q^m \partial_p^n \int_{\partial\Omega_D} d\mathbf{x} D\partial_n \tilde{G}_q(\mathbf{x}, p|\mathbf{x}_0).\end{aligned}\quad (48)$$

The definitions (6) and (7a) further simplify this relation as

$$\mathbb{E}_{\mathbf{x}_0}\{[\ell_{T_0}^R]^m T_0^n\} = (-1)^{m+n} \lim_{\substack{q \rightarrow 0 \\ p \rightarrow 0}} \partial_q^m \partial_p^n \tilde{J}_q^D(p|\mathbf{x}_0). \quad (49)$$

Note that this relation is also applicable for $m = 0$, in which case it reduces to the standard expression for the moments of the first-passage time T_0 :

$$\mathbb{E}_{\mathbf{x}_0}\{T_0^n\} = (-1)^n \lim_{p \rightarrow 0} \partial_p^n \tilde{J}_0^D(p|\mathbf{x}_0). \quad (50)$$

Like $\tilde{J}_0^D(p|\mathbf{x}_0)$ was known to be the generating function of the first-passage time T_0 , $\tilde{J}_q^D(p|\mathbf{x}_0)$ turns out to be the generating function of both T_0 and $\ell_{T_0}^R$. This is not surprising given that p and q appear as the conjugate variables in the Laplace

transforms with respect to t and ℓ . The elegant relation (49) highlights the similarity between the physical time t , which can be seen as a proxy for the number of ‘‘elementary jumps’’ of the particle in the bulk, and the boundary local time ℓ , which is a proxy of the number of its ‘‘jumps’’ on the target region $\partial\Omega_R$. This similarity was already discussed in Ref. [64] and particularly in Ref. [81], in which a surface-hopping propagator, based on the boundary local time, was introduced.

E. Reaction events

Now we can inspect the restriction of the probability flux density $j(\mathbf{x}, \ell, t|\mathbf{x}_0)$ to the target region $\partial\Omega_R$. In the Laplace domain, the spectral expansion (20) implies

$$\begin{aligned}\tilde{j}(\mathbf{x}, \ell, p|\mathbf{x}_0) &= \tilde{j}_{\infty}(\mathbf{x}, p|\mathbf{x}_0)\delta(\ell) \\ &\quad - \sum_{k=0}^{\infty} [V_k^{(p)}(\mathbf{x}_0)]^* \mu_k^{(p)} v_k^{(p)}(\mathbf{x}) e^{-\mu_k^{(p)}\ell}\end{aligned}\quad (51)$$

for any $\mathbf{x} \in \partial\Omega_R$. While this relation allows one to compute this quantity, its probabilistic interpretation remains tricky, in particular, due to its negative values according to Eq. (27).

To clarify this point, we first rewrite Eq. (4a) as $DG_q(\mathbf{x}, t|\mathbf{x}_0) = j_q(\mathbf{x}, t|\mathbf{x}_0)/q$ on $\partial\Omega_R$ and take its inverse Laplace transform with respect to q to get

$$DP(\mathbf{x}, \ell, t|\mathbf{x}_0) = \int_0^{\ell} d\ell' j(\mathbf{x}, \ell', t|\mathbf{x}_0) \quad (\mathbf{x} \in \partial\Omega_R). \quad (52)$$

The probability flux density $j(\mathbf{x}, \ell', t|\mathbf{x}_0)$ on $\partial\Omega_R$ can thus also be seen as the derivative of the full propagator on $\partial\Omega_R$ with respect to ℓ . This is consistent with the boundary value problem for the full propagator discussed in Ref. [64]. In the limit $\ell \rightarrow \infty$, Eq. (52) reduces to the relation (27) because $P(\mathbf{x}, \ell, t|\mathbf{x}_0) \rightarrow 0$, i.e., the probability of getting infinitely large values of the boundary local time ℓ_t^R at a finite time t is zero. As the left-hand side of Eq. (52) is a probability density, the integral in the right-hand side is nonnegative, despite eventual negative values of $j(\mathbf{x}, \ell', t|\mathbf{x}_0)$. What does it represent?

To get its probabilistic interpretation, we introduce the first-crossing time \mathcal{T}_{ℓ} of a threshold ℓ by the boundary local time ℓ_t^R :

$$\mathcal{T}_{\ell} = \inf\{t > 0 : \ell_t^R > \ell\}. \quad (53)$$

If the particle has escaped the domain before crossing the threshold, then the first-crossing time is set to infinity. We have then

$$\mathbb{P}\{\mathcal{T}_{\ell} > t\} = \mathbb{P}\{\ell_t^R < \ell, \mathcal{T}_0 > t\} + \mathbb{P}\{\ell_{T_0}^R < \ell, T_0 < t\}. \quad (54)$$

The first term describes no crossing of the threshold ℓ when the escape occurs after time t . In turn, the second term describes the escape event before t , for which the acquired boundary local time $\ell_{T_0}^R$ remains below the threshold. The probability density of the first-crossing time reads then as

$$\begin{aligned}U(\ell, t|\mathbf{x}_0) &= -\partial_t \mathbb{P}\{\mathcal{T}_{\ell} > t\} \\ &= -\partial_t \int_0^{\ell} d\ell' \rho(\ell', t|\mathbf{x}_0) - \int_0^{\ell} d\ell' J_D(\ell', t|\mathbf{x}_0),\end{aligned}$$

where the probability density $\rho(\ell', t|\mathbf{x}_0)$ was used to evaluate the first term in Eq. (54), and the joint probability density $J_D(\ell, t|\mathbf{x}_0)$ of $\ell_{T_0}^R$ and T_0 for the second term. Note that the definition of $\rho(\ell', t|\mathbf{x}_0)$ automatically accounts for no escape up to time t . Using the continuity equation (34), we finally get

$$U(\ell, t|\mathbf{x}_0) = \int_0^\ell d\ell' J_R(\ell', t|\mathbf{x}_0). \quad (55)$$

Despite the fact that $J_R(\ell', t|\mathbf{x}_0)$ cannot be interpreted as a joint probability density [in analogy with $J_D(\ell, t|\mathbf{x}_0)$], its integral over ℓ' yields the probability density of the first-crossing time \mathcal{T}_ℓ .

According to Eq. (52), one gets another representation

$$U(\ell, t|\mathbf{x}_0) = \int_{\partial\Omega_R} d\mathbf{x} DP(\mathbf{x}, \ell, t|\mathbf{x}_0), \quad (56)$$

which was earlier derived in Ref. [64] for the particular case $\partial\Omega_R = \partial\Omega$ (i.e., without the escape region). This relation has an intuitive interpretation. Let us again consider a thin layer of width a near $\partial\Omega_R$. By definition, the integral of the full propagator $P(\mathbf{x}, \ell, t|\mathbf{x}_0)$ over $\mathbf{x} \in \partial\Omega_R$, multiplied by a and $d\ell$, is the probability of finding the particle in that layer at time t with the boundary local time ℓ_t^R belonging to $(\ell, \ell + d\ell)$. As ℓ_t^R is a nondecreasing process that increments only when $\mathbf{X}_t \in \partial\Omega_R$, the value ℓ is thus achieved for the first time at t , i.e.,

$$\begin{aligned} a d\ell \int_{\partial\Omega_R} d\mathbf{x} P(\mathbf{x}, \ell, t|\mathbf{x}_0) &= \mathbb{P}_{\mathbf{x}_0}\{\mathcal{T}_\ell \in (t, t + dt)\} \\ &= U(\ell, t|\mathbf{x}_0) dt. \end{aligned} \quad (57)$$

Since the increments $d\ell$ and dt are related as $d\ell = Ddt/a$ according to Eq. (12), one gets Eq. (56).

In the Laplace domain, Eq. (51) implies

$$\tilde{U}(\ell, p|\mathbf{x}_0) = \sum_{k=0}^{\infty} [V_k^{(p)}(\mathbf{x}_0)]^* e^{-\mu_k^{(p)}\ell} \int_{\partial\Omega_R} d\mathbf{x} v_k^{(p)}(\mathbf{x}).$$

Setting $\ell = 0$ and employing Eq. (30), one gets

$$\begin{aligned} \tilde{U}(0, p|\mathbf{x}_0) &= \sum_{k=0}^{\infty} [V_k^{(p)}(\mathbf{x}_0)]^* \int_{\partial\Omega_R} d\mathbf{x} v_k^{(p)}(\mathbf{x}) \\ &= \int_{\partial\Omega_R} d\mathbf{x} \tilde{J}_\infty(\mathbf{x}, p|\mathbf{x}_0) = \tilde{J}_\infty^R(p|\mathbf{x}_0), \end{aligned}$$

i.e.,

$$U(0, t|\mathbf{x}_0) = J_\infty^R(t|\mathbf{x}_0). \quad (58)$$

In other words, as the first crossing of the threshold $\ell = 0$ corresponds to the first arrival onto $\partial\Omega_R$, the first-crossing time \mathcal{T}_0 is simply the first-passage time to $\partial\Omega_R$ (before escaping the domain).

As earlier stressed in Ref. [64], the probability density $U(\ell, t|\mathbf{x}_0)$ of the first-crossing time is tightly related to the probability density $J_q^R(t|\mathbf{x}_0)$ of the reaction time τ_q on $\partial\Omega_R$ discussed in Sec. II A. In fact, using Eqs. (7b), (35a), and (36), we first get

$$J_q^R(t|\mathbf{x}_0) = \int_0^\infty d\ell e^{-q\ell} J_R(\ell, t|\mathbf{x}_0). \quad (59)$$

To transform $J_R(\ell, t|\mathbf{x}_0)$ into $U(\ell, t|\mathbf{x}_0)$, one needs to integrate by parts. However, $J_R(\ell, t|\mathbf{x}_0)$ contains a singular term $J_\infty^R(t|\mathbf{x}_0)\delta(\ell)$ that has to be treated separately. We have then

$$\begin{aligned} J_q^R(t|\mathbf{x}_0) &= J_\infty^R(t|\mathbf{x}_0) + \int_{0^+}^\infty d\ell e^{-q\ell} J_R(\ell, t|\mathbf{x}_0) \\ &= J_\infty^R(t|\mathbf{x}_0) + \underbrace{\left(\int_{0^+}^\infty d\ell e^{-q\ell} U(\ell, t|\mathbf{x}_0) \right)}_{-U(0, t|\mathbf{x}_0)} \Big|_{\ell=0}^\infty \\ &\quad + q \int_{0^+}^\infty d\ell e^{-q\ell} U(\ell, t|\mathbf{x}_0), \end{aligned}$$

where we wrote the lower bound of the integral as 0^+ to highlight that the singular term was excluded. According to Eq. (58), the first two terms cancel each other, yielding

$$J_q^R(t|\mathbf{x}_0) = \int_0^\infty d\ell q e^{-q\ell} U(\ell, t|\mathbf{x}_0). \quad (60)$$

To interpret this relation, we introduce a random threshold $\hat{\ell}$ obeying the exponential probability law with the rate q , $\mathbb{P}\{\hat{\ell} > \ell\} = e^{-q\ell}$, so that $q e^{-q\ell}$ is the probability density of this law. As a consequence, the integral (60) is the average over random realizations of the threshold $\hat{\ell}$ of the probability density of the first-crossing time $\mathcal{T}_{\hat{\ell}}$. Since the left-hand side is the probability density of the reaction time τ_q , we conclude that

$$\tau_q = \mathcal{T}_{\hat{\ell}} = \inf\{t > 0 : \ell_t^R > \hat{\ell}\}, \quad (61)$$

i.e., the reaction occurs when the boundary local time ℓ_t^R exceeds the random threshold $\hat{\ell}$ with the exponential law. We emphasize that the exponential law follows directly from the postulated Robin boundary condition (4a). This interpretation, earlier suggested in Ref. [64], allows one to go beyond the Robin boundary condition and to implement various surface reaction mechanisms by choosing an appropriate law for the random threshold $\hat{\ell}$. In this way, our definition (61) of the reaction time τ_q remains valid in a much more general setting, while Eq. (60), which was specific to the Robin boundary condition, is then generalized to

$$J_\psi^R(t|\mathbf{x}_0) = \int_0^\infty d\ell \psi(\ell) U(\ell, t|\mathbf{x}_0), \quad (62)$$

where $\psi(\ell)$ is the chosen probability density of the random threshold $\hat{\ell}$. Different choices of $\psi(\ell)$ and its consequences on the distribution of the reaction time were discussed in Ref. [64]. This extension of surface reaction mechanisms is directly applicable to our setting with the escape region $\partial\Omega_D$. In this way, we made a step further toward more realistic modeling of diffusion-controlled reactions by incorporating the effect of escape events.

We complete this section by providing a deeper probabilistic interpretation of the first-passage time T_q to the escape region $\partial\Omega_D$ in the presence of the reactive region $\partial\Omega_R$. As discussed in Sec. II A, this random variable is described by the probability density $J_q^D(t|\mathbf{x}_0)$, which is related to $J_D(\ell, t|\mathbf{x}_0)$ due to Eq. (36) as

$$J_q^D(t|\mathbf{x}_0) = \int_0^\infty d\ell e^{-q\ell} J_D(\ell, t|\mathbf{x}_0). \quad (63)$$

As previously, the factor $e^{-q\ell}$ incorporates the condition of no reaction until the escape, which was automatically included into the left-hand side via the Robin boundary condition on $\partial\Omega_R$. In turn, if the reaction happens before the escape, then the escape time T_q is set to infinity. In other words, one has

$$T_q = \begin{cases} T_0 & \text{if } \ell_{T_0}^R < \hat{\ell}, \\ +\infty & \text{otherwise.} \end{cases} \quad (64)$$

As earlier, the dependence on the reactivity parameter q is incorporated via the random threshold $\hat{\ell}$ obeying the exponential law with the rate q . This representation highlights the effect of surface reactions onto the first-passage time T_q . In fact, if the target region $\partial\Omega_R$ was inert, then the particle would reach the escape region $\partial\Omega_D$ at a random time T_0 . In turn, the reactivity of $\partial\Omega_R$ makes the only change that the particle can react on $\partial\Omega_R$ and thus never escape. If the boundary local time $\ell_{T_0}^R$ at T_0 has not crossed the random threshold $\hat{\ell}$, then the reaction on $\partial\Omega_R$ has not happened, and $T_q = T_0$. In contrast, if the threshold $\hat{\ell}$ has been crossed, then the reaction occurred before T_0 so that $T_q = \infty$. The above definition of the first-passage time to the escape region $\partial\Omega_D$ within the encounter-based approach allows one to study this quantity for other surface reaction mechanisms, beyond the conventional one described by Robin boundary condition. For this purpose, one can choose an appropriate law $\mathbb{P}\{\hat{\ell} > \ell\}$ for the random threshold $\hat{\ell}$ and replace the factor $e^{-q\ell}$ in Eq. (63) by this law. Further investigations of this setting present an interesting perspective of the present work.

III. SPHERICAL TARGET

To illustrate the general properties of diffusion-controlled reactions with eventual escape, we consider diffusion between two concentric spheres of radii R and L : $\Omega = \{\mathbf{x} \in \mathbb{R}^3 : R < |\mathbf{x}| < L\}$. The inner sphere represents the target region $\partial\Omega_R$, while the outer sphere is the escape region $\partial\Omega_D$ (in this setting, $\partial\Omega_N = \emptyset$). In spherical coordinates $\mathbf{x} = (r, \theta, \phi)$, the

modified Helmholtz equation can be solved via separation of variables. In particular, the eigenbasis of the Dirichlet-to-Neumann operator is well known [71,81,82]. In fact, the rotational invariance of the domain implies that the eigenfunctions of \mathcal{M}_p are the (normalized) spherical harmonics $Y_{nm}(\theta, \phi)$,

$$v_{nm} = \frac{1}{R} Y_{nm}(\theta, \phi) \quad \left(\begin{array}{l} n = 0, 1, \dots, \\ |m| \leq n \end{array} \right), \quad (65)$$

where the double index nm is used instead of a single index k . In turn, the eigenvalues are

$$\mu_{nm}^{(p)} = -(\partial_r g_n^{(p)}(r))_{r=R}, \quad (66)$$

where

$$g_n^{(p)}(r) = \frac{k_n(\alpha L) i_n(\alpha r) - i_n(\alpha L) k_n(\alpha r)}{k_n(\alpha L) i_n(\alpha R) - i_n(\alpha L) k_n(\alpha R)} \quad (67)$$

are the radial functions, with $\alpha = \sqrt{p/D}$ and $i_n(z)$ and $k_n(z)$ being the modified spherical Bessel functions of the first and second kind. Note that $g_n^{(p)}(L) = 0$ and $g_n^{(p)}(R) = 1$. One sees that the eigenvalues are $(2n+1)$ times degenerate (they do not depend on the index m), while the eigenfunctions do not depend on p . Finally, it is easy to check that

$$V_{nm}^{(p)}(\mathbf{x}) = g_n^{(p)}(r) v_{nm}(\theta, \phi). \quad (68)$$

As most quantities of interest are obtained by integrating over the target region $\partial\Omega_R$, the orthogonality of eigenfunctions v_{nm} to $v_{00} = 1/\sqrt{4\pi R^2}$ ensures that all terms vanish except this ground eigenmode. Since $i_0(z) = \sinh(z)/z$ and $k_0(z) = e^{-z}/z$, one finds

$$g_0^{(p)}(r) = \frac{R \sinh[\alpha(L-r)]}{r \sinh[\alpha(L-R)]} \quad (69)$$

and

$$\mu_0^{(p)} = \mu_{00}^{(p)} = \frac{1}{R} + \alpha \operatorname{ctanh}[\alpha(L-R)]. \quad (70)$$

Note that

$$\int_{\Omega} d\mathbf{x} V_{00}^{(p)}(\mathbf{x}) = \frac{4\pi}{\sqrt{4\pi R^2}} \int_R^L dr r^2 g_0^{(p)}(r) = \frac{\sqrt{4\pi}}{\sinh[\alpha(L-R)]} \left\{ -\frac{L}{\alpha} + \frac{\alpha R \cosh[\alpha(L-R)] + \sinh[\alpha(L-R)]}{\alpha^2} \right\}$$

and

$$C_0^{(p)} = \sqrt{4\pi} \frac{\alpha L}{\sinh[\alpha(L-R)]}.$$

One can also compute

$$J_q^D(p|\mathbf{x}_0) = \frac{L}{r_0} \frac{(1+qR) \sinh[\alpha(r_0-R)] + \alpha R \cosh[\alpha(r_0-R)]}{(1+qR) \sinh[\alpha(L-R)] + \alpha R \cosh[\alpha(L-R)]}, \quad (71a)$$

$$J_q^R(p|\mathbf{x}_0) = \frac{R}{r_0} \frac{qR \sinh(\alpha(L-r_0))}{(1+qR) \sinh[\alpha(L-R)] + \alpha R \cosh[\alpha(L-R)]}, \quad (71b)$$

where $r_0 = |\mathbf{x}_0|$, from which

$$J_{\infty}^R(p|\mathbf{x}_0) = \frac{R \sinh[\alpha(L-r_0)]}{r_0 \sinh[\alpha(L-R)]}, \quad J_{\infty}^D(p|\mathbf{x}_0) = \frac{L \sinh[\alpha(r_0-R)]}{r_0 \sinh[\alpha(L-R)]}, \quad J_0^D(p|\mathbf{x}_0) = \frac{L}{r_0} \frac{\sinh[\alpha(r_0-R)] + \alpha R \cosh[\alpha(r_0-R)]}{\sinh[\alpha(L-R)] + \alpha R \cosh[\alpha(L-R)]}.$$

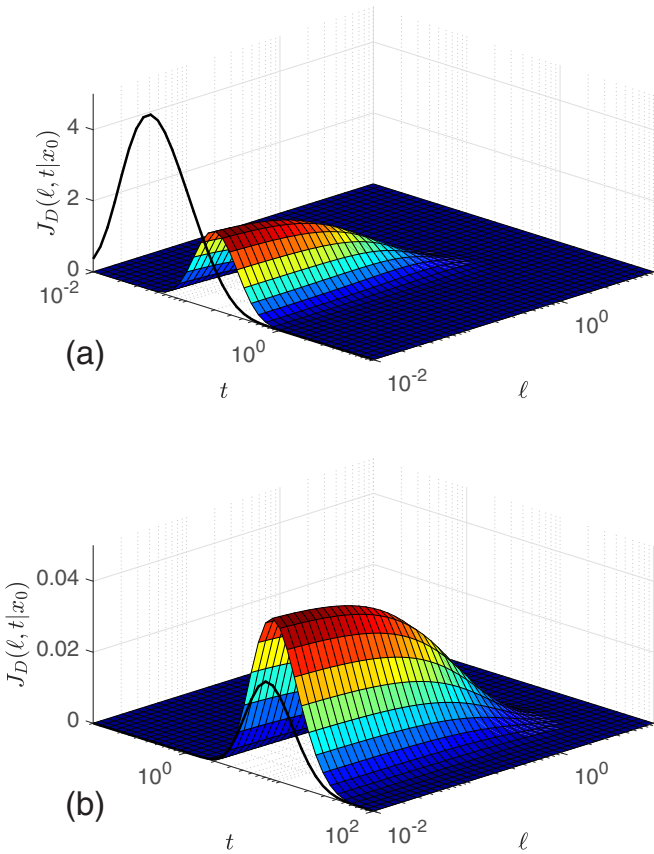


FIG. 2. Joint probability density $J_D(\ell, t|\mathbf{x}_0)$ of the boundary local time $\ell_{T_0}^R$ and the escape time T_0 for diffusion between two concentric spheres of radii R and L , with $R = 1$, $r_0 = 1.5$, $D = 1$, $L = 2$ (a) and $L = 10$ (b). Surface shows the regular part of this density, while black solid line presents the prefactor $J_\infty^D(t|\mathbf{x}_0)$ in front of the singular term $\delta(\ell)$. Note that this curve should be located at $\ell = 0$, which is not visible on the logarithmic scale; it was thus artificially put at $\ell = 10^{-2}$ for illustration purposes. The ranges of times t differ by factor 10 between two panels.

In the following illustrations, we fix units of length and time by setting $R = 1$ and $D = 1$.

A. Escape events

According to Eq. (38), we find

$$\begin{aligned} \tilde{J}_D(\ell, p|\mathbf{x}_0) &= \frac{L \sinh[\alpha(r_0 - R)]}{r_0 \sinh[\alpha(L - R)]} \delta(\ell) \\ &+ \frac{L \alpha \sinh[\alpha(L - r_0)]}{r_0 \sinh^2[\alpha(L - R)]} e^{-\mu_0^{(p)} \ell}, \end{aligned} \quad (73)$$

from which an inverse Laplace transform with respect to p yields the joint probability density $J_D(\ell, t|\mathbf{x}_0)$ of $\ell_{T_0}^R$ and T_0 . The inversion of the first term in Eq. (73) can be found explicitly via the residue theorem. In turn, the presence of the p -dependent factor $e^{-\mu_0^{(p)} \ell}$ in the second term makes the inversion challenging (see Ref. [71] for some analytical tools). For this reason, we employed a numerical Laplace transform inversion by the Talbot algorithm [83].

Figure 2 illustrates the behavior of $J_D(\ell, t|\mathbf{x}_0)$. Two terms in Eq. (73) give respectively singular and regular contributions

to this density with respect to ℓ . The regular contribution as a function of ℓ and t is shown by a surface. In turn, the singular contribution corresponding to $\ell = 0$ is shown by a black line. For Fig. 2(a), we set $L = 2$ and $r_0 = 1.5$, i.e., the particle starts in the middle between the target region at $R = 1$ and the escape region at $L = 2$; in turn, in Fig. 2(b), the escape region is moved to $L = 10$.

Since the particle needs to diffuse from its starting point \mathbf{x}_0 to the escape region at L , its escape at very short times is highly unlikely. In particular, the probability density $J_\infty^D(t|\mathbf{x}_0)$ of the first-passage time to $\partial\Omega_D$ determining the singular term, is known to exhibit the short-time behavior of a Lévy-Smirnov form $t^{-3/2} e^{-(L-r_0)^2/(4Dt)}$ (see Refs. [84,85] and references therein). Similar behavior can be derived for the regular contribution. In the same vein, the probability of escape at very long times is also negligible because the particle cannot avoid the escape region too long. These arguments explain a distinct maximum of $J_D(\ell, t|\mathbf{x}_0)$ with respect to t at intermediate times. Finally, too large values of the boundary local time $\ell_{T_0}^R$ for intermediate escape times would require for the particle to stay too long near the target region $\partial\Omega_R$, which is also highly improbable. One sees therefore that $J_\infty^D(t|\mathbf{x}_0)$ exhibits a single “boss” that rapidly goes down as $t \rightarrow 0$, $t \rightarrow \infty$, or $\ell \rightarrow \infty$.

Figure 2(a) indicates that the maximum of the singular contribution [the curve $J_\infty^D(t|\mathbf{x}_0)$] is shifted to shorter times with respect to the boss of $J_D(\ell, t|\mathbf{x}_0)$. In fact, the particle that never hit the target region $\partial\Omega_R$ (and thus has $\ell_{T_0}^R = 0$) needs to travel the distance $L - r_0$ from the starting point to the escape region that determines the maximum of $J_\infty^D(t|\mathbf{x}_0)$. In turn, the particle that first encountered $\partial\Omega_R$ and then escaped, has to travel the longer distance $(r_0 - R) + (L - R)$ that requires longer time. When the starting point gets closer to $\partial\Omega_D$, the separation between two maxima is even larger, while the location of \mathbf{x}_0 near $\partial\Omega_R$ would reduce this separation. Similarly, if L is much larger than r_0 [as on Fig. 2(b)], then the difference between two distances is relatively small, and two maxima are close.

Setting $p = 0$ in Eq. (73), one gets the (marginal) probability density of $\ell_{T_0}^R$:

$$\begin{aligned} \rho_D(\ell|\mathbf{x}_0) &= \frac{L}{r_0(L - R)} \left\{ (r_0 - R) \delta(\ell) + \frac{L - r_0}{L - R} e^{-\ell[1/R + 1/(L - R)]} \right\}. \end{aligned} \quad (74)$$

This is a mixture of an exponential distribution and an atom at $\ell = 0$. Figure 3 illustrates the regular (exponential) part of this distribution for the example from Fig. 2(a). As an additional validation step, we also realized Monte Carlo simulations of random trajectories and thus independently evaluated the statistics of $\ell_{T_0}^R$. For this purpose, a random trajectory of a particle was simulated by adding independent Gaussian increments, with mean zero and variance $\sqrt{2D\delta}$ in each direction, where δ is a small time step. If the particle jumps inside the inner sphere of radius R , then it is normally reflected back. At each step when the particle is within a layer of width a near the inner sphere (i.e., when $|X_t| < R + a$), the boundary local time ℓ_t^R is incremented by $D\delta/a$ according to Eq. (12). The simulation is stopped when the particle crosses the outer sphere of radius L . Repeating such a simulation M times, one

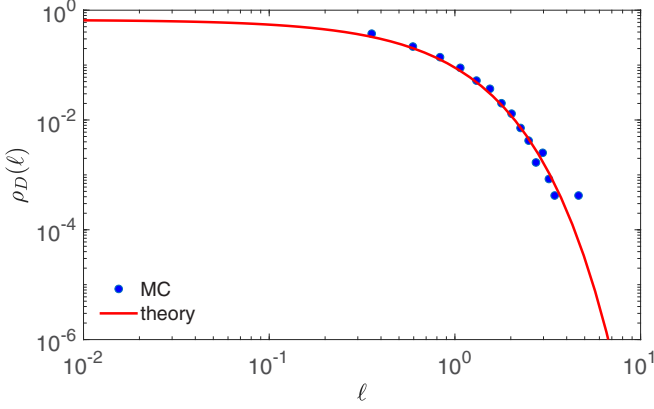


FIG. 3. The regular part of the probability density $\rho_D(\ell|\mathbf{x}_0)$ of the acquired boundary local time $\ell_{T_0}^R$ up to the escape time T_0 for diffusion between two concentric spheres of radii R and L , with $R = 1$, $L = 2$, $r_0 = 1.5$, and $D = 1$. Solid line shows the exact solution (74), while symbols present a renormalized histogram from Monte Carlo simulations with $M = 10^4$ particles, the time step $\delta = 10^{-4}$ and the layer width $a = 5\sqrt{2D\delta}$.

gets an empirical statistics of the escape time T_0 and of the acquires boundary local time $\ell_{T_0}^R$.

Figure 3 confirms an excellent agreement between the exact solution (74) and simulations. One can also appreciate that getting the behavior of $\rho_D(\ell|\mathbf{x}_0)$ at too small or too large ℓ is problematic for Monte Carlo simulations. In fact, estimations at small ℓ require very short time steps in the modeling of the random trajectory (and thus too long simulations). In turn, estimations at large ℓ require too many simulated trajectories, as the probability of getting large $\ell_{T_0}^R$ is exponentially small.

The moments of $\ell_{T_0}^R$ are particularly simple:

$$\mathbb{E}_{\mathbf{x}_0}\{[\ell_{T_0}^R]^m\} = m! \frac{R(L-r_0)}{r_0(L-R)} \left(\frac{1}{R} + \frac{1}{L-R}\right)^{-m}. \quad (75)$$

In particular,

$$\mathbb{E}_{\mathbf{x}_0}\{\ell_{T_0}^R\} = R^2(1/r_0 - 1/L), \quad (76a)$$

$$\mathbb{V}_{\mathbf{x}_0}\{\ell_{T_0}^R\} = R^3(1/r_0 - 1/L)(2 - R/r_0 - R/L), \quad (76b)$$

where $\mathbb{V}_{\mathbf{x}_0}$ denotes the variance. The moments of T_0 are determined via Eq. (50); in particular, one has

$$\mathbb{E}_{\mathbf{x}_0}\{T_0\} = \frac{(L-r_0)[r_0L(r_0+L) - 2R^3]}{6Dr_0L} \quad (77)$$

and

$$\begin{aligned} \mathbb{V}_{\mathbf{x}_0}\{T_0\} = & \frac{L-r_0}{90D^2L^2r_0^2} (r_0^2L^5 + L^4r_0^3 + r_0^4L^3 + r_0^5L^2 \\ & - 20L^2r_0^2R^3 + 36R^5r_0L - 10R^6L - 10R^6r_0). \end{aligned} \quad (78)$$

In turn, the joint moments can be found from

$$\begin{aligned} \mathbb{E}_{\mathbf{x}_0}\{[\ell_{T_0}^R]^m T_0^n\} = & (-1)^n m! \frac{L}{r_0} \\ & \times \lim_{p \rightarrow 0} \frac{\partial^n}{\partial p^n} \left\{ \frac{\alpha \sinh[\alpha(L-r_0)]}{\sinh^2[\alpha(L-R)]} [\mu_0^{(p)}]^{-m-1} \right\}. \end{aligned} \quad (79)$$

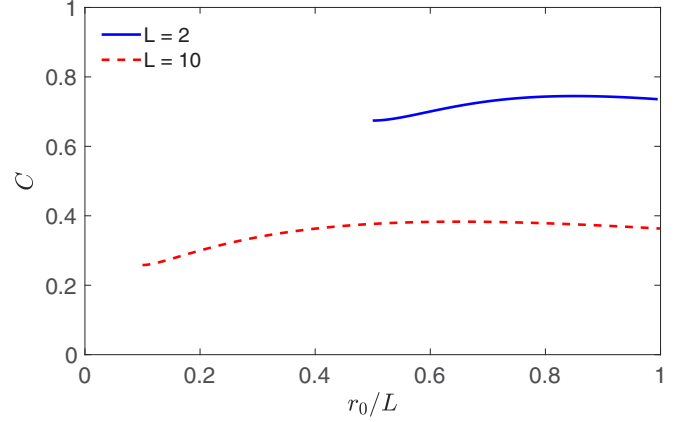


FIG. 4. The correlation coefficient between the escape time T_0 and the boundary local time $\ell_{T_0}^R$ as a function of r_0/L , for diffusion between two concentric spheres of radii R and L , with $R = 1$, $D = 1$, and two values of L indicated in the legend.

For instance, we get

$$\mathbb{E}_{\mathbf{x}_0}\{\ell_{T_0}^R T_0\} = \frac{R^2(L-r_0)}{6DL^2r_0} [2(L+2R)(L-R)^2 - L(L-r_0)^2]. \quad (80)$$

Expectedly, all these quantities vanish as $r_0 \rightarrow L$ because the particle started on $\partial\Omega_D$ escapes immediately, yielding $T_0 = \ell_{T_0}^R = 0$ in a deterministic way. The above expressions allow one to compute the Pearson's correlation coefficient between T_0 and $\ell_{T_0}^R$:

$$C = \frac{\mathbb{E}_{\mathbf{x}_0}\{\ell_{T_0}^R T_0\} - \mathbb{E}_{\mathbf{x}_0}\{\ell_{T_0}^R\} \mathbb{E}_{\mathbf{x}_0}\{T_0\}}{\sqrt{\mathbb{V}_{\mathbf{x}_0}\{T_0\}} \sqrt{\mathbb{V}_{\mathbf{x}_0}\{\ell_{T_0}^R\}}}. \quad (81)$$

Figure 4 shows the correlation coefficient C as a function of r_0/L for two values of L . In both cases, the correlation is positive. Indeed, if the particle escapes faster (at smaller T_0), then it would generally have lower chances to encounter the target region frequently so that the boundary local time $\ell_{T_0}^R$ would also be smaller. Note that correlations are higher for the case $L = 2$ than for $L = 10$. In other words, when the distance between the escape and target regions is larger, the particle would generally take longer time to diffuse in the confining domain before the escape and thus to decorrelate these random variables. Even though all moments vanish as $r_0 \rightarrow L$, the correlation coefficient gets a nontrivial limit. Curiously, both curves exhibit slightly nonmonotonous behavior with respect to r_0 .

B. First-crossing times

According to Eq. (51), we have

$$\tilde{J}_R(\ell, p|\mathbf{x}_0) = g_0(r_0) [\delta(\ell) - \mu_0^{(p)} e^{-\mu_0^{(p)} \ell}], \quad (82)$$

and thus

$$\tilde{U}(\ell, p|\mathbf{x}_0) = g_0(r_0) e^{-\mu_0^{(p)} \ell}. \quad (83)$$

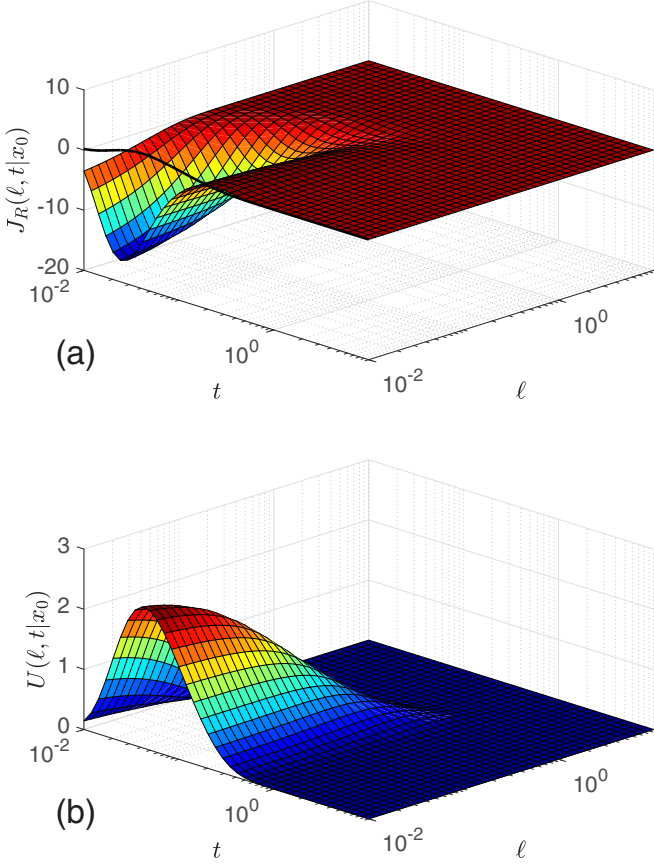


FIG. 5. (a) Probability flux density $J_R(\ell, t|\mathbf{x}_0)$ for diffusion between two concentric spheres of radii R and L , with $R = 1$, $L = 2$, $r_0 = 1.5$, and $D = 1$. Surface shows the regular part of this density, which was obtained by the numerical Laplace transform inversion of Eq. (82) with respect to p by Talbot algorithm. Black solid line presents the prefactor $J_\infty^R(t|\mathbf{x}_0)$ in front of the singular term $\delta(\ell)$. Note that this curve should be located at $\ell = 0$, which is not visible on the logarithmic scale; it was thus artificially put at $\ell = 10^{-2}$ for illustration purposes. (b) Probability density $U(\ell, t|\mathbf{x}_0)$ of the first-crossing time \mathcal{T}_ℓ for the same setting. This density is obtained by the numerical Laplace transform inversion of Eq. (83) with respect to p by Talbot algorithm. According to Eq. (55), $J_R(\ell, t|\mathbf{x}_0)$ is the derivative of $U(\ell, t|\mathbf{x}_0)$ with respect to ℓ .

Figure 5(a) illustrates the behavior of $J_R(\ell, t|\mathbf{x}_0)$. As previously, we plot the regular and singular parts by a surface and a black curve. In sharp contrast to $J_D(\ell, t|\mathbf{x}_0)$ shown on Fig. 2, the regular part of $J_R(\ell, t|\mathbf{x}_0)$ is negative, as discussed in Sec. II E. Moreover, the minimum of the regular part is not shifted with respect to the maximum of the singular term $J_\infty^R(t|\mathbf{x}_0)$. This is related to the fact that both extrema are determined by the time needed for the particle to travel from \mathbf{x}_0 to the target region at R . Interestingly, the “amplitude” of the regular part of $J_R(\ell, t|\mathbf{x}_0)$ is an order of magnitude higher than that of $J_D(\ell, t|\mathbf{x}_0)$. In particular, the black curve showing $J_\infty^R(t|\mathbf{x}_0)$ looks almost flat at this scale. This observation does not contradict Eq. (55) that ensures the positivity of the integral of $J_R(\ell', t|\mathbf{x}_0)$ over ℓ' from 0 to any ℓ . This is confirmed by Fig. 5(b) showing this integral. For each value of the threshold ℓ , this figure gives the probability density $U(\ell, t|\mathbf{x}_0)$ of the first-crossing time \mathcal{T}_ℓ . We recall that this density is not

normalized to 1 due to escape events:

$$\int_0^\infty dt U(\ell, t|\mathbf{x}_0) = \tilde{U}(\ell, 0|\mathbf{x}_0) = \frac{R(L - r_0)}{r_0(L - R)} e^{-\ell/[1/R+1/(L-R)]} \leq 1. \quad (84)$$

The probability density $U(\ell, t|\mathbf{x}_0)$ as a function of both ℓ and t exhibits a single “boss”; in fact, it is unlikely to cross a given threshold ℓ at too short or too long times; in turn, the decrease at large ℓ is ensured by the normalization relation (84). Even though the shape of $U(\ell, t|\mathbf{x}_0)$ looks similar to that of $J_D(\ell, t|\mathbf{x}_0)$ shown on Fig. 2, their probabilistic interpretations are different.

Yet another difference between $J_D(\ell, t|\mathbf{x}_0)$ and $J_R(\ell, t|\mathbf{x}_0)$ is that the former strongly depends on the location of the escape region (compare two panels of Fig. 2), whereas the latter exhibits only a weak dependence on L whenever L is large enough. For this reason, we do not present the graphs of $J_R(\ell, t|\mathbf{x}_0)$ and $U(\ell, t|\mathbf{x}_0)$ for $L = 10$, because they are almost indistinguishable from that shown on Fig. 5 for $L = 2$. This can be seen from Eq. (83): when $\sqrt{p/D}(L - r_0) \gg 1$, one has

$$\tilde{U}(\ell, p|\mathbf{x}_0) \approx \frac{R}{r_0} e^{-(r_0 - R + \ell)\sqrt{p/D} - \ell/R}, \quad (85)$$

which is independent of L . Its inverse Laplace transform yields

$$U(\ell, t|\mathbf{x}_0) \approx \frac{R e^{-\ell/R}}{r_0} \frac{(r_0 - R + \ell) e^{-(r_0 - R + \ell)^2/(4Dt)}}{\sqrt{4\pi Dt^3}}. \quad (86)$$

The right-hand side is actually the exact form of the probability density $U(\ell, t|\mathbf{x}_0)$ for a spherical target in the three-dimensional space (i.e., in the limit $L \rightarrow \infty$), as reported in Ref. [81]. As the approximation (85) fails in the limit $p \rightarrow 0$ [in which case $\sqrt{p/D}(L - r_0) \gg 1$ cannot hold], the approximation (86) fails at long times. This is expected because if the particle has enough time to explore the domain Ω , it will unavoidably hit the escape region.

Figure 6 allows one to compare the probability density $U(\ell, t|\mathbf{x}_0)$ for a particular value $\ell = 1$ with the results of Monte Carlo simulations. One observes an excellent agreement between the theory and simulations. This figure also highlights the difficulty in getting the values of $U(\ell, t|\mathbf{x}_0)$ at short and long times by Monte Carlo simulations. We also plot the approximation (86) in the limit $L \rightarrow \infty$. As said earlier, this approximation is very accurate at short times but fails at long times. As L increases, the validity range of the approximation progressively extends to longer and longer times.

IV. CONCLUSION

In this paper, we revised the encounter-based approach to diffusion-mediated surface phenomena and generalized this formalism by allowing a generic partition of the boundary $\partial\Omega$ into three parts: a target region $\partial\Omega_R$, a reflecting region $\partial\Omega_N$ and an escape region $\partial\Omega_D$. While the original formulation in Ref. [64] dealt with the whole boundary as the target ($\partial\Omega = \partial\Omega_R$), our generalization brings a greater flexibility to modeling diffusion-controlled reactions and covers a broad scope of related first-passage problems. From the

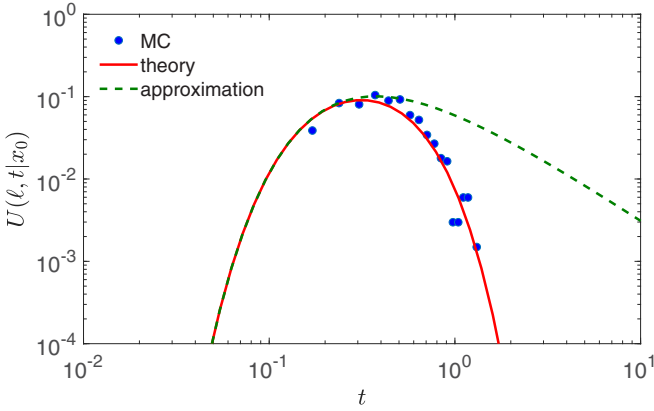


FIG. 6. Probability density $U(\ell, t|\mathbf{x}_0)$ of the first-crossing time \mathcal{T}_ℓ of a threshold ℓ by the boundary local time ℓ_t^R for diffusion between two concentric spheres of radii R and L , with $R = 1$, $L = 2$, $r_0 = 1.5$, $D = 1$, and $\ell = 1$. Symbols present a renormalized histogram from Monte Carlo simulations with $M = 10^4$, $\delta = 10^{-4}$ and $a = 5\sqrt{2D\delta}$, solid line shows the numerical Laplace transform inversion of Eq. (83) by Talbot algorithm, while dashed line indicates the approximation (86) corresponding to the limit $L \rightarrow \infty$.

mathematical point of view, this extension essentially consists in adding Neumann and Dirichlet boundary conditions on $\partial\Omega_N$ and $\partial\Omega_D$, respectively. Despite this apparent simplicity, the inclusion of a “killing mechanism” for the diffusing particle (an escape through $\partial\Omega_D$) has required some conceptual refinements and appropriate modifications in the formalism. In particular, we focused in the paper on the probability flux density $j(\mathbf{x}, \ell, t|\mathbf{x}_0)$, which was mostly ignored in former works.

On the one hand, the restriction of $j(\mathbf{x}, \ell, t|\mathbf{x}_0)$ to the escape region $\partial\Omega_D$ determined, for the first time, the joint probability density of the escape time T_0 , the particle position \mathbf{X}_{T_0} , and the acquired boundary local time $\ell_{T_0}^R$ on the target region $\partial\Omega_R$. In turn, the marginal density $J_D(\ell, t|\mathbf{x}_0)$, in which the position \mathbf{X}_{T_0} was averaged out, allows one to characterize not only the statistics of the number of encounters between the target region and the diffusing particle before its escape, but also correlations with the escape time. In particular, we obtained the three equivalent representations (44), (48), and (49) of the joint moments of $\ell_{T_0}^R$ and T_0 and revealed a probabilistic interpretation of multiple derivatives of the Green’s function $\tilde{G}_q(\mathbf{x}, p|\mathbf{x}_0)$ with respect to p and q . Note that earlier works dealt exclusively with the escape time itself and were mainly focused on the mean value and its dependence on the geometric and kinetic parameters. However, it is important to emphasize that the mean escape time, which is mostly affected by long but rare trajectories, may be orders of magnitude larger than the typical time of the escape process, and thus be noninformative or even misleading [85–89]. For instance, this may occur when the particle starts in a neighborhood of a small escape region. In this situation, the whole distribution of the escape time (or another quantity such as $\ell_{T_0}^R$) is needed to characterize the escape process. For this reason, we focused on the probability flux densities that were much less studied in the past.

On the other hand, the restriction of $j(\mathbf{x}, \ell, t|\mathbf{x}_0)$ to the target region $\partial\Omega_R$ required a subtle probabilistic interpretation

in terms of the first-crossing time \mathcal{T}_ℓ of a given threshold ℓ by the boundary local time ℓ_t^R . In particular, the integral of $j(\mathbf{x}, \ell', t|\mathbf{x}_0)$ over $\mathbf{x} \in \partial\Omega_R$ and over ℓ' from 0 to ℓ determined the probability density $U(\ell, t|\mathbf{x}_0)$ of \mathcal{T}_ℓ . The latter played a key role in the generalization of conventional surface reactions, described by the Robin boundary condition, to more general mechanisms. While this generalization was already presented in Ref. [64], its extension in the presence of escape events required some refinements. For instance, the former derivation relied on the nondecreasing character of the boundary local time ℓ_t and its immediate consequence that $\mathbb{P}\{\mathcal{T}_\ell > t\} = \mathbb{P}\{\ell_t < \ell\}$. In the presence of the escape region, this relation has to be replaced by Eq. (54) accounting for the value $\mathcal{T}_\ell = \infty$ in the case if the particle has escaped before crossing the threshold ℓ . More generally, the lack of a proper normalization of probability densities had to be carefully managed.

For illustrative purposes, we considered diffusion between concentric spheres, the inner sphere of radius R being the target region and the outer sphere of radius L being the escape region. This basic example allowed us to compute all the discussed quantities in a simple compact form in the Laplace domain and then to evaluate the inverse Laplace transform numerically. We presented both $J_D(\ell, t|\mathbf{x}_0)$ and $J_R(\ell, t|\mathbf{x}_0)$, as well as some derived quantities such as $\rho_D(\ell|\mathbf{x}_0)$ and $U(\ell, t|\mathbf{x}_0)$. We discussed two cases: $L = 2$ (when the target and escape regions are relatively close to each other), and $L = 10$ (when they are well separated). Expectedly, the joint probability density $J_D(\ell, t|\mathbf{x}_0)$ strongly depends on the location of the escape region, whereas $J_R(\ell, t|\mathbf{x}_0)$ showed only a weak dependence on L . In particular, the probability density $U(\ell, t|\mathbf{x}_0)$ approaches the well-known explicit form (86) for a spherical target in the three-dimensional space.

While we considered ordinary diffusion inside the confining domain, the presented formalism allows one to easily incorporate a first-order reaction kinetics in the bulk. This kinetics may account for a spontaneous disappearance of the diffusing particle (or its “activity”) with a constant rate γ due to radioactive disintegration, photobleaching, relaxation of its excited state, disassembly, failure, or biological death. Whatever the actual killing mechanism, such a “mortal” particle can be treated as having a random lifetime δ that obeys the exponential law $\mathbb{P}\{\delta > t\} = e^{-\gamma t}$ [90–93]. In the conventional approach, the killing mechanism in the bulk is included by adding the term $-\gamma G_q(\mathbf{x}, t|\mathbf{x}_0)$ to the right-hand side of the diffusion equation (1). Its Laplace transform with respect to t yields the same modified Helmholtz equation (19), in which p is replaced by $p' = p + \gamma$. As a consequence, most results that we obtained in the Laplace domain, remain valid up to this trivial change. Moreover, many Laplace-transformed quantities, evaluated at $p = \gamma$, admit useful probabilistic interpretations in terms of the stopping condition at the “death” time δ . For instance,

$$\gamma \tilde{\rho}(\ell, \gamma|\mathbf{x}_0) = \int_0^\infty dt \gamma e^{-\gamma t} \rho(\ell, t|\mathbf{x}_0) \quad (87)$$

is the probability density of the boundary local time ℓ_δ^R at the random time δ of the particle “death” in the bulk, with $\gamma e^{-\gamma t}$ being the probability density of δ . In other words, many Laplace-transformed quantities that we

derived in this paper, have their own interest, even without evaluating their inverse Laplace transforms. The combined effect of the first-order kinetics in the bulk, surface reactions on the target region, and escape events can be further explored.

The present work can be extended in several directions. On the mathematical side, the spectral properties of the Dirichlet-to-Neumann operator need further attention. In addition to a rigorous demonstration of the announced basic properties, the asymptotic behavior of the eigenvalues $\mu_k^{(p)}$ has to be uncovered, in particular, in the limit when either $\partial\Omega_R$ or $\partial\Omega_D$ (or both) is small. We expect that some matched asymptotic tools [94,95] can be adapted to investigate this problem. On the application side, one can

investigate in more detail the effect of escape events onto various surface reaction mechanisms introduced in Ref. [64]. The proposed extension can be further analyzed in the presence of multiple independently diffusing particles [96], eventual resetting mechanisms [97–99] and drifts [100]. Future applications of the extended encounter-based approach can bring more realistic features to a theoretical description of biology-inspired transport processes, notably in living cells.

ACKNOWLEDGMENT

The author thanks the Alexander von Humboldt Foundation for support through the Bessel Prize award.

- [1] B. Alberts, A. Johnson, J. Lewis, D. Morgan, M. Raff, K. Roberts, and P. Walter, *Molecular Biology of the Cell* (Garland Science, New York, NY, 2014).
- [2] S. A. Rice, *Diffusion-Limited Reactions* (Elsevier, Amsterdam, 1985).
- [3] D. A. Lauffenburger and J. Linderman, *Receptors: Models for Binding, Trafficking, and Signaling* (Oxford University Press, Oxford, UK, 1993).
- [4] Z. Schuss, *Brownian Dynamics at Boundaries and Interfaces in Physics, Chemistry and Biology* (Springer, New York, NY, 2013).
- [5] K. Lindenberg, R. Metzler, and G. Oshanin, *Chemical Kinetics: Beyond the Textbook* (World Scientific, New Jersey, 2019).
- [6] P. C. Bressloff and J. M. Newby, Stochastic models of intracellular transport, *Rev. Mod. Phys.* **85**, 135 (2013).
- [7] S. Redner, *A Guide to First Passage Processes* (Cambridge University Press, Cambridge, UK, 2001).
- [8] *First-Passage Phenomena and Their Applications*, edited by R. Metzler, G. Oshanin, and S. Redner (World Scientific, Singapore, 2014).
- [9] S. Condamin, O. Bénichou, V. Tejedor, R. Voituriez, and J. Klafter, First-passage time in complex scale-invariant media, *Nature (London)* **450**, 77 (2007).
- [10] O. Bénichou, C. Chevalier, J. Klafter, B. Meyer, and R. Voituriez, Geometry-controlled kinetics, *Nat. Chem.* **2**, 472 (2010).
- [11] D. Holcman and Z. Schuss, Control of flux by narrow passages and hidden targets in cellular biology, *Rep. Prog. Phys.* **76**, 074601 (2013).
- [12] O. Bénichou and R. Voituriez, From first-passage times of random walks in confinement to geometry-controlled kinetics, *Phys. Rep.* **539**, 225 (2014).
- [13] D. S. Grebenkov, Universal Formula for the Mean First Passage Time in Planar Domains, *Phys. Rev. Lett.* **117**, 260201 (2016).
- [14] T. Guérin, N. Levernier, O. Bénichou, and R. Voituriez, Mean first-passage times of non-Markovian random walkers in confinement, *Nature (London)* **534**, 356 (2016).
- [15] Y. Lanoiselée, N. Moutal, and D. S. Grebenkov, Diffusion-limited reactions in dynamic heterogeneous media, *Nat. Commun.* **9**, 4398 (2018).
- [16] C. W. Gardiner, *Handbook of Stochastic Methods for Physics, Chemistry, and the Natural Sciences* (Springer, Berlin, 1985).
- [17] N. G. Van Kampen, *Stochastic Processes in Physics and Chemistry* (Elsevier, Amsterdam, 1992).
- [18] F. C. Collins and G. E. Kimball, Diffusion-controlled reaction rates, *J. Colloid Sci.* **4**, 425 (1949).
- [19] H. C. Berg and E. M. Purcell, Physics of chemoreception, *Biophys. J.* **20**, 193 (1977).
- [20] H. Sano and M. Tachiya, Partially diffusion-controlled recombination, *J. Chem. Phys.* **71**, 1276 (1979).
- [21] K. R. Brownstein and C. E. Tarr, Importance of classical diffusion in NMR studies of water in biological cells, *Phys. Rev. A* **19**, 2446 (1979).
- [22] G. H. Weiss, Overview of theoretical models for reaction rates, *J. Stat. Phys.* **42**, 3 (1986).
- [23] J. G. Powles, M. J. D. Mallett, G. Rickayzen, and W. A. B. Evans, Exact analytic solutions for diffusion impeded by an infinite array of partially permeable barriers, *Proc. R. Soc. London A* **436**, 391 (1992).
- [24] B. Sapoval, General Formulation of Laplacian Transfer Across Irregular Surfaces, *Phys. Rev. Lett.* **73**, 3314 (1994).
- [25] B. Sapoval, M. Filoche, and E. Weibel, Smaller is better—but not too small: A physical scale for the design of the mammalian pulmonary acinus, *Proc. Natl. Acad. Sci. USA* **99**, 10411 (2002).
- [26] D. S. Grebenkov, M. Filoche, B. Sapoval, and M. Felici, Diffusion-Reaction in Branched Structures: Theory and Application to the Lung Acinus, *Phys. Rev. Lett.* **94**, 050602 (2005).
- [27] S. D. Traytak and W. Price, Exact solution for anisotropic diffusion-controlled reactions with partially reflecting conditions, *J. Chem. Phys.* **127**, 184508 (2007).
- [28] P. C. Bressloff, B. A. Earnshaw, and M. J. Ward, Diffusion of protein receptors on a cylindrical dendritic membrane with partially absorbing traps, *SIAM J. Appl. Math.* **68**, 1223 (2008).
- [29] A. Singer, Z. Schuss, A. Osipov, and D. Holcman, Partially reflected diffusion, *SIAM J. Appl. Math.* **68**, 844 (2008).
- [30] D. S. Grebenkov, Searching for partially reactive sites: Analytical results for spherical targets, *J. Chem. Phys.* **132**, 034104 (2010).
- [31] S. D. Lawley and J. P. Keener, A new derivation of Robin boundary conditions through homogenization of a stochastically switching boundary, *SIAM J. Appl. Dyn. Syst.* **14**, 1845 (2015).
- [32] D. S. Grebenkov, Analytical representations of the spread harmonic measure density, *Phys. Rev. E* **91**, 052108 (2015).

- [33] A. S. Serov, C. Salafia, D. S. Grebenkov, and M. Filoche, The role of morphology in mathematical models of placental gas exchange, *J. Appl. Physiol.* **120**, 17 (2016).
- [34] P. C. Bressloff, Stochastic switching in biology: From genotype to phenotype, *J. Phys. A: Math. Theor.* **50**, 133001 (2017).
- [35] D. S. Grebenkov and G. Oshanin, Diffusive escape through a narrow opening: New insights into a classic problem, *Phys. Chem. Chem. Phys.* **19**, 2723 (2017).
- [36] F. Piazza and D. S. Grebenkov, Diffusion-controlled reaction rate on nonspherical partially absorbing axisymmetric surfaces, *Phys. Chem. Chem. Phys.* **21**, 25896 (2019).
- [37] D. S. Grebenkov, Spectral theory of imperfect diffusion-controlled reactions on heterogeneous catalytic surfaces, *J. Chem. Phys.* **151**, 104108 (2019).
- [38] H. S. Carslaw and J. C. Jaeger, *Conduction of Heat in Solids*, 2nd ed. (Oxford University Press, Oxford, UK, 1959).
- [39] J. Crank, *The Mathematics of Diffusion* (Oxford University Press, Oxford, UK, 1956).
- [40] R. K. M. Thambynayagam, *The Diffusion Handbook: Applied Solutions for Engineers* (McGraw Hill, New York, NY, 2011).
- [41] D. S. Grebenkov and B.-T. Nguyen, Geometrical structure of Laplacian eigenfunctions, *SIAM Rev.* **55**, 601 (2013).
- [42] V. G. Maz'ya, S. A. Nazarov, and B. A. Plamenevskii, Asymptotic expansions of the eigenvalues of boundary value problems for the Laplace operator in domains with small holes, *Math. USSR Izv.* **24**, 321 (1985).
- [43] M. J. Ward and J. B. Keller, Strong localized perturbations of eigenvalue problems, *SIAM J. Appl. Math.* **53**, 770 (1993).
- [44] T. Kolokolnikov, M. S. Titcombe, and M. J. Ward, Optimizing the fundamental Neumann eigenvalue for the Laplacian in a domain with small traps, *Eur. J. Appl. Math* **16**, 161 (2005).
- [45] A. Singer, Z. Schuss, D. Holcman, and R. S. Eisenberg, Narrow escape, Part I, *J. Stat. Phys.* **122**, 437 (2006).
- [46] A. Singer, Z. Schuss, and D. Holcman, Narrow escape, Part II: The circular disk, *J. Stat. Phys.* **122**, 465 (2006).
- [47] A. Singer, Z. Schuss, and D. Holcman, Narrow escape, Part III: Nonsmooth domains and Riemann surfaces, *J. Stat. Phys.* **122**, 491 (2006).
- [48] Z. Schuss, A. Singer, and D. Holcman, The narrow escape problem for diffusion in cellular microdomains, *Proc. Natl. Acad. Sci. USA* **104**, 16098 (2007).
- [49] O. Bénichou and R. Voituriez, Narrow-Escape Time Problem: Time Needed for a Particle to Exit a Confining Domain Through a Small Window, *Phys. Rev. Lett.* **100**, 168105 (2008).
- [50] S. Pillay, M. J. Ward, A. Peirce, and T. Kolokolnikov, An asymptotic analysis of the mean first passage time for narrow escape problems: Part I: Two-dimensional domains, *Multiscale Model. Simul.* **8**, 803 (2010).
- [51] A. F. Cheviakov, M. J. Ward, and R. Straube, An asymptotic analysis of the mean first passage time for narrow escape problems: Part II: The sphere, *Multiscale Model. Simul.* **8**, 836 (2010).
- [52] A. F. Cheviakov and M. J. Ward, Optimizing the principal eigenvalue of the Laplacian in a sphere with interior traps, *Math. Comput. Model.* **53**, 1394 (2011).
- [53] A. F. Cheviakov, A. S. Reimer, and M. J. Ward, Mathematical modeling and numerical computation of narrow escape problems, *Phys. Rev. E* **85**, 021131 (2012).
- [54] D. Holeman and Z. Schuss, The narrow escape problem, *SIAM Rev.* **56**, 213 (2014).
- [55] T. Agranov and B. Meerson, Narrow Escape of Interacting Diffusing Particles, *Phys. Rev. Lett.* **120**, 120601 (2018).
- [56] D. S. Grebenkov, R. Metzler, and G. Oshanin, Full distribution of first exit times in the narrow escape problem, *New J. Phys.* **21**, 122001 (2019).
- [57] S. D. Traytak, The diffusive interaction in diffusion-limited reactions: The steady-state case, *Chem. Phys. Lett.* **197**, 247 (1992).
- [58] S. Condamin and O. Bénichou, Exact expressions of mean first-passage times and splitting probabilities for random walks in bounded rectangular domains, *J. Chem. Phys.* **124**, 206103 (2006).
- [59] C. Chevalier, O. Bénichou, B. Meyer and R. Voituriez, First-passage quantities of Brownian motion in a bounded domain with multiple targets: A unified approach, *J. Phys. A: Math. Theor.* **44**, 025002 (2011).
- [60] M. Galanti, D. Fanelli, S. D. Traytak, and F. Piazza, Theory of diffusion-influenced reactions in complex geometries, *Phys. Chem. Chem. Phys.* **18**, 15950 (2016).
- [61] D. S. Grebenkov and S. Traytak, Semi-analytical computation of Laplacian Green functions in three-dimensional domains with disconnected spherical boundaries, *J. Comput. Phys.* **379**, 91 (2019).
- [62] D. S. Grebenkov, Diffusion toward non-overlapping partially reactive spherical traps: Fresh insights onto classic problems, *J. Chem. Phys.* **152**, 244108 (2020).
- [63] J. Klinger, R. Voituriez, and O. Bénichou, Splitting Probabilities of Symmetric Jump Processes, *Phys. Rev. Lett.* **129**, 140603 (2022).
- [64] D. S. Grebenkov, Paradigm Shift in Diffusion-Mediated Surface Phenomena, *Phys. Rev. Lett.* **125**, 078102 (2020).
- [65] P. Lévy, *Processus Stochastiques et Mouvement Brownien* (Gauthier-Villard, Paris, 1965).
- [66] K. Itô and H. P. McKean, *Diffusion Processes and Their Sample Paths* (Springer, Berlin, 1965).
- [67] M. Freidlin, *Functional Integration and Partial Differential Equations*, Annals of Mathematics Studies (Princeton University Press, Princeton, NJ, 1985).
- [68] A. N. Borodin and P. Salminen, *Handbook of Brownian Motion: Facts and Formulae* (Birkhauser Verlag, Basel, Boston, Berlin, 1996).
- [69] S. N. Majumdar, Brownian functionals in physics and computer science, *Curr. Sci.* **89**, 2076 (2005).
- [70] D. S. Grebenkov, Statistics of boundary encounters by a particle diffusing outside a compact planar domain, *J. Phys. A: Math. Theor.* **54**, 015003 (2021).
- [71] D. S. Grebenkov, Joint distribution of multiple boundary local times and related first-passage time problems with multiple targets, *J. Stat. Mech.* (2020) 103205.
- [72] W. Arendt, A. F. M. ter Elst, J. B. Kennedy, and M. Sauter, The Dirichlet-to-Neumann operator via hidden compactness, *J. Funct. Anal.* **266**, 1757 (2014).
- [73] D. Daners, Non-positivity of the semigroup generated by the Dirichlet-to-Neumann operator, *Positivity* **18**, 235 (2014).
- [74] A. F. M. ter Elst and E. M. Ouhabaz, Analysis of the heat kernel of the Dirichlet-to-Neumann operator, *J. Funct. Anal.* **267**, 4066 (2014).

- [75] J. Behrndt and A. F. M. ter Elst, Dirichlet-to-Neumann maps on bounded Lipschitz domains, *J. Diff. Equ.* **259**, 5903 (2015).
- [76] W. Arendt and A. F. M. ter Elst, The Dirichlet-to-Neumann operator on exterior domains, *Potential Anal.* **43**, 313 (2015).
- [77] A. Hassell and V. Ivrii, Spectral asymptotics for the semiclassical Dirichlet to Neumann operator, *J. Spectr. Theory* **7**, 881 (2017).
- [78] A. Girouard and I. Polterovich, Spectral geometry of the Steklov problem, *J. Spectr. Theory* **7**, 321 (2017).
- [79] D. S. Grebenkov, Probability distribution of the boundary local time of reflected Brownian motion in Euclidean domains, *Phys. Rev. E* **100**, 062110 (2019).
- [80] P. Mörters and Y. Peres, *Brownian Motion*, Cambridge Series in Statistical and Probabilistic Mathematics (Cambridge University Press, New York, NY, 2010).
- [81] D. S. Grebenkov, Surface hopping propagator: An alternative approach to diffusion-influenced reactions, *Phys. Rev. E* **102**, 032125 (2020).
- [82] D. S. Grebenkov, Statistics of diffusive encounters with a small target: Three complementary approaches, *J. Stat. Mech.* (2022) 083205.
- [83] A. Talbot, The accurate numerical inversion of Laplace transforms, *IMA J. Appl. Math.* **23**, 97 (1979).
- [84] A. Godec and R. Metzler, Universal Proximity Effect in Target Search Kinetics in the Few-Encounter Limit, *Phys. Rev. X* **6**, 041037 (2016).
- [85] D. S. Grebenkov, R. Metzler, and G. Oshanin, Strong defocusing of molecular reaction times results from an interplay of geometry and reaction control, *Commun. Chem.* **1**, 96 (2018).
- [86] T. G. Mattos, C. Mejia-Monasterio, R. Metzler, and G. Oshanin, First passages in bounded domains: When is the mean first passage time meaningful? *Phys. Rev. E* **86**, 031143 (2012).
- [87] A. Godec and R. Metzler, First passage time distribution in heterogeneity controlled kinetics: Going beyond the mean first passage time, *Sci. Rep.* **6**, 20349 (2016).
- [88] D. S. Grebenkov, R. Metzler, and G. Oshanin, Towards a full quantitative description of single-molecule reaction kinetics in biological cells, *Phys. Chem. Chem. Phys.* **20**, 16393 (2018).
- [89] M. Reva, D. A. DiGregorio, and D. S. Grebenkov, A first-passage approach to diffusion-influenced reversible binding: Insights into nanoscale signaling at the presynapse, *Sci. Rep.* **11**, 5377 (2021).
- [90] S. B. Yuste, E. Abad, and K. Lindenberg, Exploration and Trapping of Mortal Random Walkers, *Phys. Rev. Lett.* **110**, 220603 (2013).
- [91] B. Meerson and S. Redner, Mortality, Redundancy, and Diversity in Stochastic Search, *Phys. Rev. Lett.* **114**, 198101 (2015).
- [92] D. S. Grebenkov and J.-F. Rupprecht, The escape problem for mortal walkers, *J. Chem. Phys.* **146**, 084106 (2017).
- [93] B. Meerson, Mortal Brownian motion: Three short stories, *Int. J. Mod. Phys. B* **33**, 1950172 (2019).
- [94] P. C. Bressloff, Diffusion-mediated absorption by partially-reactive targets: Brownian functionals and generalized propagators, *J. Phys. A: Math. Theor.* **55**, 205001 (2022).
- [95] P. C. Bressloff, Narrow capture problem: An encounter-based approach to partially reactive targets, *Phys. Rev. E* **105**, 034141 (2022).
- [96] D. S. Grebenkov, Depletion of resources by a population of diffusing species, *Phys. Rev. E* **105**, 054402 (2022).
- [97] M. R. Evans, S. N. Majumdar, and G. Schehr, Stochastic resetting and applications, *J. Phys. A: Math. Theor.* **53**, 193001 (2020).
- [98] P. C. Bressloff, Diffusion-mediated surface reactions and stochastic resetting, *J. Phys. A: Math. Theor.* **55**, 275002 (2022).
- [99] Z. Benkhadj and D. S. Grebenkov, Encounter-based approach to diffusion with resetting, *Phys. Rev. E* **106**, 044121 (2022).
- [100] D. S. Grebenkov, An encounter-based approach for restricted diffusion with a gradient drift, *J. Phys. A: Math. Theor.* **55**, 045203 (2022).